Cretaceous Research 138 (2022) 105275

Contents lists available at ScienceDirect

Cretaceous Research

journal homepage: www.elsevier.com/locate/CretRes

Temporal constraints on the terrestrial biota from the Yingzuilazi Formation (Baishan Basin), northeast China

Yaqiong Wang [a,*], Yuting Zhong [b,c]

[a] State Key Laboratory of Palaeobiology and Stratigraphy, Nanjing Institute of Geology and Palaeontology and Center for Excellence in Life and Paleoenvironment, Chinese Academy of Sciences, 39 East Beijing Road, Nanjing 210008, China
[b] State Key Laboratory of Isotope Geochemistry, Guangzhou Institute of Geochemistry, Chinese Academy of Sciences, Guangzhou 510640, China
[c] CAS Center for Excellence in Deep Earth Science, Guangzhou 510640, China

ARTICLE INFO

Article history:
Received 11 April 2022
Received in revised form
25 May 2022
Accepted in revised form 5 June 2022
Available online 13 June 2022

Keywords:
Ostracoda
Cypridea
Ziziphocypris
Zircon U–Pb dating
North China Craton
Barremian

ABSTRACT

The biota from the Yingzuilazi Formation in the Baishan Basin yields a diverse fossil assemblage (including a new described ostracod species *Cypridea horni* sp. nov. Wang), which provides a valuable opportunity to investigate the evolution of major terrestrial plants and animals. However, the age of this biota is still controversial. To address this, we report a new SIMS zircon U–Pb age of 128.5 ± 1.0 Ma for the uppermost part of the Yingzuilazi Formation. This age, combined with our new ostracod biostratigraphic age from the Yingzuilazi Formation, indicate that the age of biota from the Yingzuilazi Formation is mainly Barremian (~129 Ma to ~127 Ma). It seems that the biota from the Yingzuilazi Formation temporal coincides with Jehol Biota *sensu stricto* stage I, but it is closely related to Jehol Biota *sensu stricto* stage II in terms of comprehensive biostratigraphic and paleontoloical materials. Therefore, this biota shows the significances not only in understanding the spatiotemporal evolution of the Early Cretaceous terrestrial biotas in East Asia, but also in exploring the possible relationship between the terrestrial life evolution and the destruction processes of the North China Craton.

1. Introduction

Non-marine Jurassic to Cretaceous sedimentary rocks are widely exposed in China, especially in northeast China where two world-famous Mesozoic terrestrial Lagersätten are discovered: The Middle–Late Jurassic Yanliao Biota and the Early Cretaceous Jehol Biota (e.g. Zhou and Wang, 2017; Xi et al., 2019; Xu et al., 2020; Zhou et al., 2021). In recent year, an increasing number of research indicated that the spatiotemporal evolution of the Yanliao and Jehol biotas coincided with the initial and peak stages of the North China Craton (NCC) destruction, respectively (e.g. Zhu et al., 2012a,b, 2020; Zhou and Wang, 2017; Xu et al., 2020; Zhou et al., 2021). Therefore, the northeast China especially the NCC is the ideal place to explore the linkage of terrestrial life evolution and the deep dynamic processes of the earth (e.g. Zhu et al., 2020; Zhou et al., 2021). Besides the Yanliao and Jehol biotas, several other biotas have also been found in northeast China especially in NCC, which are contemporaneous and have the same geological background with the former two biotas (Zhou et al., 2021), such as the biota from the Yingzuilazi Formation of the Baishan Basin (Huang, 2016; Li et al., 2018). These biotas are thought as the supplementary data to discuss the evolution of terrestrial life as well as the possible relationship between terrestrial life evolution and tectonic processes (Zhou et al., 2021). Previously, the biota from the Yingzuilazi Formation was assigned to the Late Jurassic (Bureau of Geology and Mineral Resources of Jilin Province, 1988, 1997 and also see the geological map of Hunjiang (1:200, 000)), whereas some recent studies suggested that the biota from the Yingzuilazi Formation belongs to the Early Cretaceous Jehol Biota (Huang, 2016; Li et al., 2018; Guo et al., 2018). To date, no absolute age has been reported for the Yingzuilazi Formation, which has hindered attempts to define the age of biota from this formation.

In this study, we report a new zircon U–Pb SIMS age from the volcanic ash in the uppermost part of the Yingzuilazi Formation. Meanwhile, a biostratigraphy framework is established based on the new discovered non-marine ostracod fauna of the Yingzuila Formation. These new data provide a critical age constraint for the Yingzuilazi Formation via two independent methods. Therefore,

* Corresponding author.
E-mail address: yqwang@nigpas.ac.cn (Y. Wang).

https://doi.org/10.1016/j.cretres.2022.105275
0195-6671/

this work provides a robust chronostratigraphic framework for the biota from the Yingzuilazi Formation in the Baishan Basin.

2. Geological setting

The Baishan Basin (= "the Hunjiang Basin") is one of the small typical rift basins in northeast China, which is situated in the northeast margin area of the NCC (Huang, 2016; Chen et al., 2016; Guo et al., 2018; Meng et al., 2021) (Fig. 1). It is surrounded by the Tianshan–Xingmeng orogenic belt to the north, the Liaodong Peninsula to the south and the Korean Peninsula to the east (Chen et al., 2016). The Cretaceous sedimentary sequences of this basin divide into four formations in ascending order: Yingzuilazi, Linzitou, Shiren and Yumuqiaozi formations (Fig. 1). Of these, the

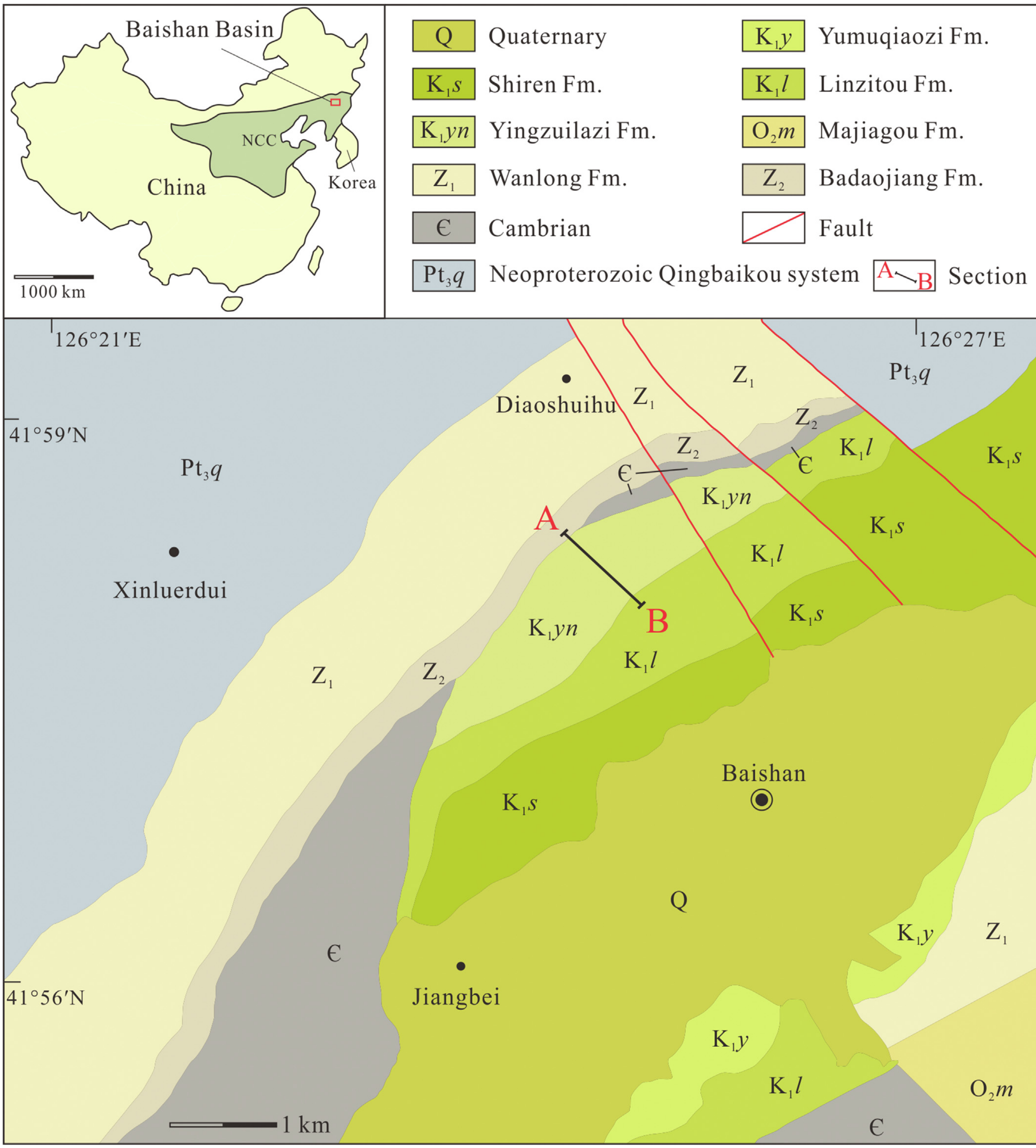

Fig. 1. The location map. The inset map showing the location of the Baishan Basin in the North China Carton within China (NCC= North China Carton) (modified from the 1:200, 000 geological map of Hunjiang area and Zhu et al., 2012b, fig. 1).

Yingzuilazi Formation yields a diverse flora and abundant lacustrine and terrestrial invertebrates and vertebrates (e.g. Li et al., 2015; Huang, 2016; Zhao et al., 2016; Li et al., 2018; Guo et al., 2018).

The studied section closed to Yingzuilazi village (Baishan city, Jinlin Province; Fig. 1) is regarded as the stratotype section of the Yingzuilazi Formation (e.g. Li et al., 2015; Huang, 2016). Detailed stratigraphic descriptions were given by Huang (2016). The Yingzuilazi Formation is dominated by lacustrine depositional sequences consisting of conglomerate, sandstone, siltstone, shale, and coal (Fig. 2). It unconformably overlies the Proterozoic Badaojiang Formation, and is overlain by the Linzitou Formation (Li et al., 2015).

3. Material and method

3.1. Tuff sample

Sample YZLZ-02 was collected from a variegated gray tuff layer that is ~35 cm thick (41°58′21″ N, 126°25′52″ E), located at the uppermost part of the Yingzuilazi Formation (Figs. 2 and 3A). Thin sections were made for petrographic studies. It is a poorly sorted crystal tuff. The crystal fragments are dominated by angular to subangular quartz (10–150 μm) and feldspar (20–100 μm) (Fig. 3B–D). Some bright yellow and elongated biotites were observed (Fig. 3B).

3.2. Zircon U–Pb dating by SIMS

Zircons were separated from the tuff sample YZLZ-02 using conventional heavy liquid and magnetic techniques and purified by hand-picking under a binocular microscope. About 200 grains were mounted on epoxy mount and the internal structures of the zircon were exposed by polish the mount to half section for analyses. Zircons were documented transmitted and reflected light photomicrographs as well as cathodoluminescence (CL) images to reveal their external and internal structures. CL images were obtained using a Supra 55 Sapphire (Carl Zeiss Company, Germany) field emission scanning electron microscope (FESEM) connected to a MonoCL4 system (Gatan Company, UK) at the State Key Laboratory of Isotope Geochemistry (SKLIG), Guangzhou Institute of Geochemistry, Chinese Academy of Sciences (GIGCAS) (Guangzhou, China). The imaging conditions were 10 kV with a working distance of 14.9 mm. The analyzed spot should be located by checking the CL images with transmitted and reflected light photomicrographs that the appropriate target sites could avoid cracks and inclusions of zircon crystals.

Zircon U–Pb dating were performed on a CAMECA IMS1280-HR system at the SKLIG, GIGCAS. The analytical procedure was similar to that reported by Li et al. (2009). A primary O_2^- ion beam of ~8 nA was used to bombard the surface of selected zircon, with a 20 μm × 30 μm ion spot size. Each measurement consisted of seven cycles, and the total analytical time was ca. 12 min. Standard analyses were obtained after every five unknown analyses. The zircon standard Plešovice (Sláma et al., 2008) was analyzed to calibrate Pb/U ratios based on the linear relationship between $\ln(^{206}Pb/^{238}U)$ and $\ln(^{238}U^{16}O_2/^{238}U)$ (Whitehouse et al., 1997). Uncertainties on single analyses are reported at the 1σ level. The data reduction was carried out by use of the Geochronology software developed at NORDSIM by Dr. Martin Whitehouse. The data processing concept is equivalent to SQUID. The plotting program Isoplot/Ex_ver4.15 (Ludwig, 2011) was used to calculate ages, uncertainties, weighted means, and the generation of U–Pb concordia plots. A reference zircon SA01 (Huang et al., 2020) was analyzed as unknown to monitor the reliability of the whole procedure. Five measurements of SA01 yielded a $^{206}Pb/^{238}U$ age of 535.2 ± 8.8 Ma (1σ), which is consistent within errors with the reported value of 535.08 ± 0.32 Ma (Huang et al., 2020).

3.3. Ostracod samples

The studied ostracod samples were collected from the Yingzuilazi Formation at the Yingzuilazi section (41°58′33″ N, 126°25′56″ E) (Fig. 2). We totally collected fifteen samples. Of these, thirteen samples contain ostracod individuals, and two samples only contain ostracod fragments. The rock samples (250 g for each) were crushed 1 cm × 1 cm pieces, then were kept in an oven at 60 °C for 24 h. After drying the samples were totally covered with warm water and 5% surfactant liquid. Two days later, the samples were washed under 2 mm and 0.063 mm meshes. The fine deposit fragments which lift on the 0.063 mm mesh were dried again. Ostracod specimens were picked under a binocular microscope. Ostracod carapaces/valves are coated gold and scanned with Hitachi SU3500 scanning electron microscopes at the Nanjing Institute of Geology and Palaeontology, Chinese Academy of Sciences (NIGPAS) (Nanjing, China). The figured specimens are housed in the Nanjing Institute of Geology and Palaeontology, Chinese Academy of Sciences (NIGPAS) under the collection numbers NIGP 176368–176434.

4. Results

4.1. Zircon U–Pb geochronology

Zircon grains are abundant in the tuff sample YZLZ-02, enabling precise U–Pb age determination. Zircons from this sample are mostly euhedral and 100–200 μm in length with length to width ratios varying from 3 to 6. Most grains are clear in color, and showing oscillatory magmatic zoning in CL images (Fig. 4), indicating a magmatic origin (Corfu et al., 2003). U–Pb isotopic ratios and ages that were obtained by SIMS are listed in Supplementary Table 1. A total of 24 zircon crystals were analyzed. U and Th contents vary from 145 to 640 ppm and from 81 to 490 ppm, respectively. The Th/U ratios of analyzed zircons range from 0.36 to 1.11. Twenty-one spot analyses of zircons from YZLZ-02 are concordant, with $^{206}Pb/^{238}U$ and $^{207}Pb/^{235}U$ ages in agreement within analytical error, yielding a concordia age of 128.5 ± 1.2 Ma (Fig. 4A). Analysis 03 was excluded from the calculation because it was discordant (Fig. 4A). Besides, two grains (analyses 06 and 15) are slightly older and were thus excluded because of likely inheritance (Fig. 4A). The remaining 21 analyses yielded a weighted mean $^{206}Pb/^{238}U$ age of 128.5 ± 1.0 Ma (n = 21, MSWD = 1.05; Fig. 4B), which is interpreted as the depositional age of the tuff sample YZLZ-02.

4.2. Ostracod systematic palaeontology

The classification for suprageneric categories follows Sames (2011a,b), Danielopol et al. (2018) and Meisch et al. (2019). Abbreviations used in text and figures, H: height; L: length; W: width; LV: left valve; RV: right valve. Size intervals used are: Very small: <0.40 mm, small: 0.40–0.50 mm, medium: 0.51–0.70 mm, large: 0.71–1.00 mm, very large: 1.01–2.00 mm, gigantic: >2.0 mm (e.g. Ayress and Whatley, 2014). Morphologic terminology, Anterior and posterior outline and margin curvature symmetry: equicurvate = equally rounded; infracurvate = narrower towards ventre; supracurvate = narrower rounded towards dorsum (see Sames, 2011a,b, fig. 5 for illustration and Sames, 2011c for definitions).

Class Ostracoda Latreille, 1802
Subclass Podocopa Sars, 1866

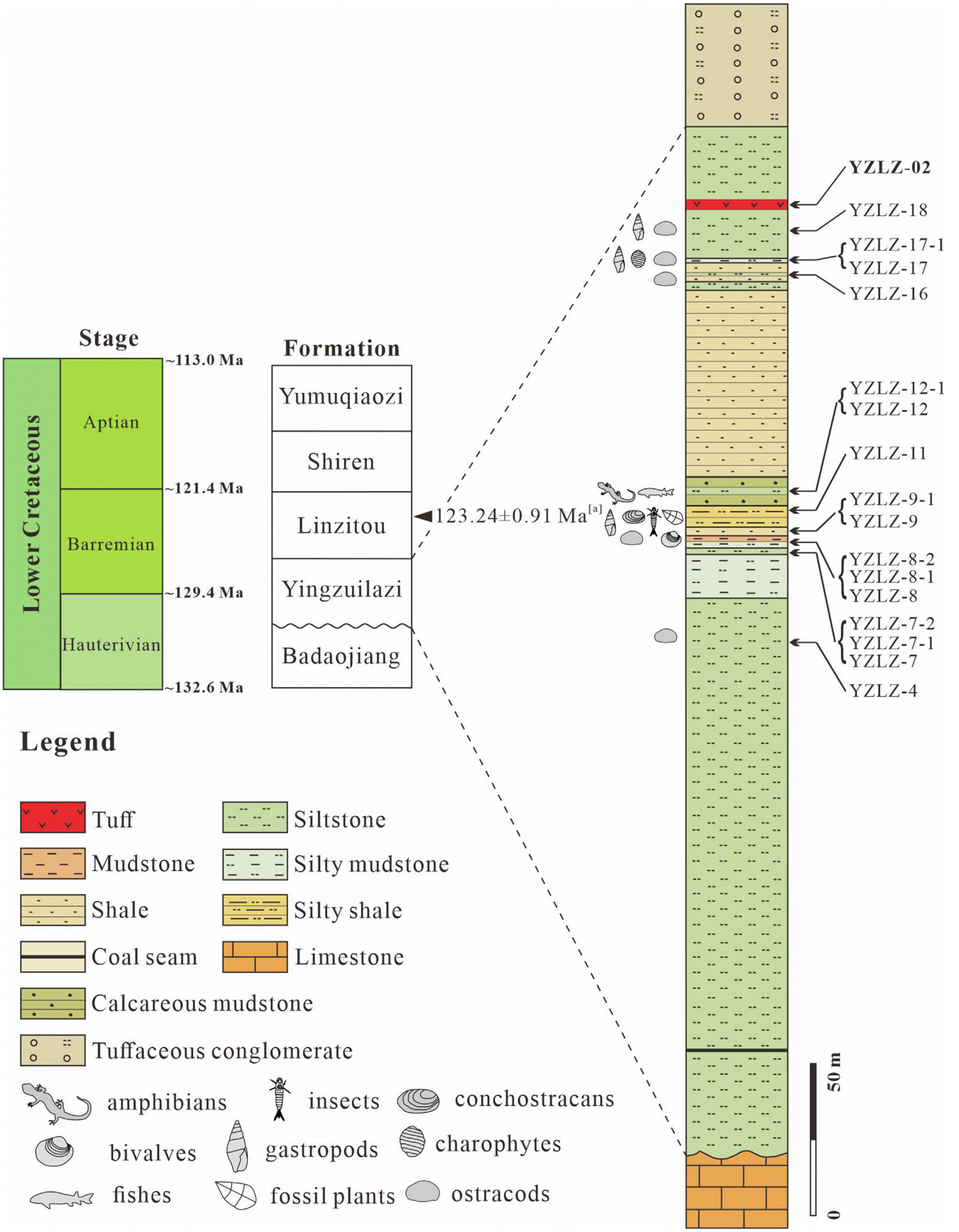

Fig. 2. Stratigraphic columns showing lithologies and the positions of the ostracod samples and tuff sample in the Yingzuilazi Formation at the Yingzuilazi section of the Baishan Basin (modified from Huang, 2016, fig. 1.4). Reference [a] Chen et al. (2016).

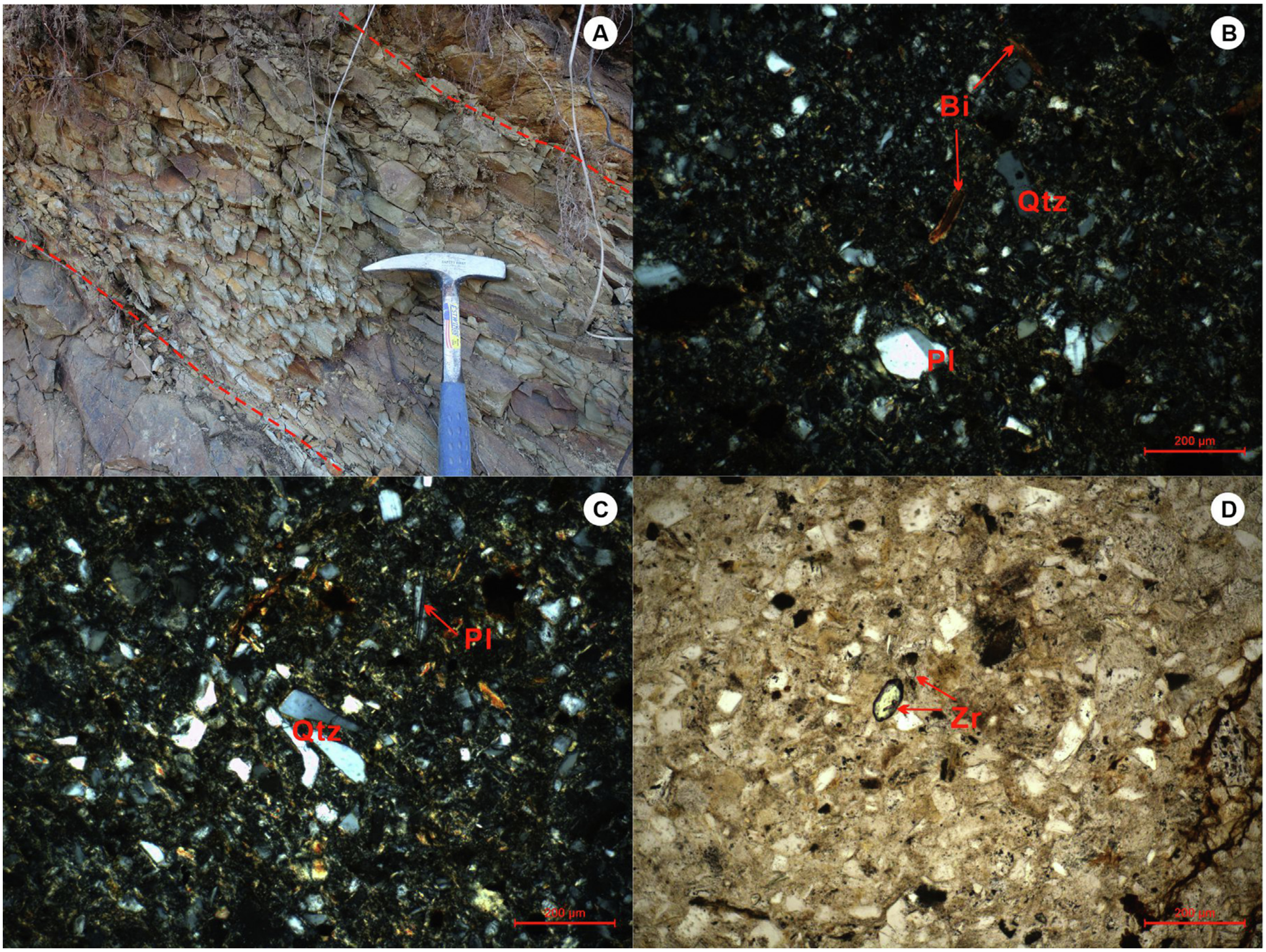

Fig. 3. A, Field occurrence of tuff sample YZLZ-02; B–C, Photomicrographs under cross-polarized light; D, Photomicrograph under plane-polarized light; Pl: plagioclase; Qtz: Quartz; Bi: Biotite; Zr: Zircon.

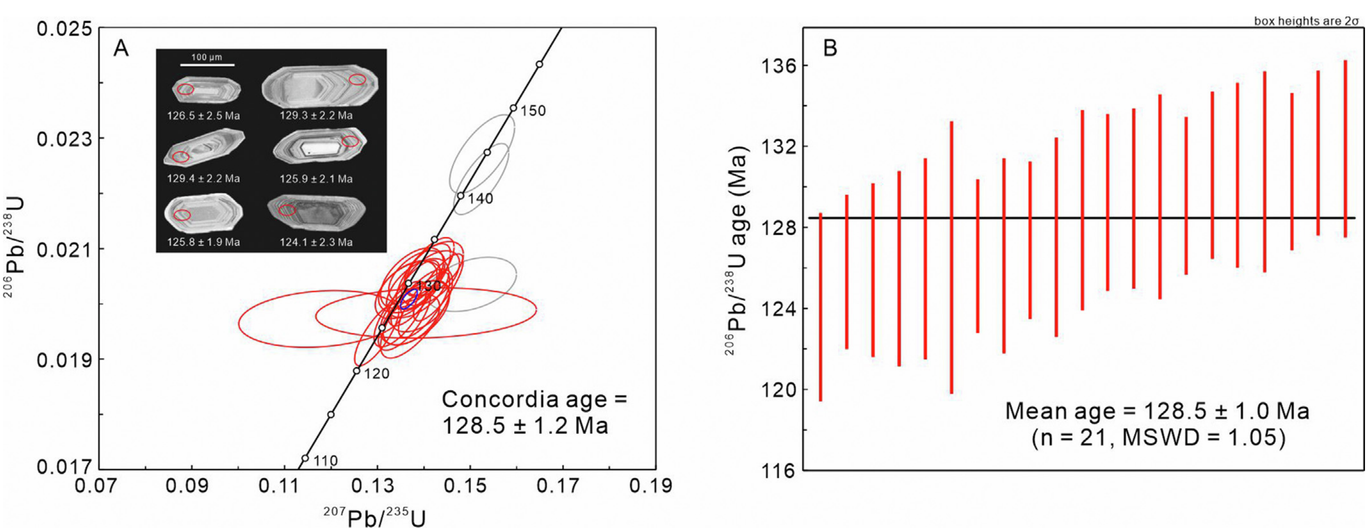

Fig. 4. (A) U–Pb Concordia diagram and (B) Plot of individual analyses show the U–Pb dating results from SIMS analyses for YZLZ-02. Inset figures are cathodoluminescence images of representative zircons. Number below each grain is the corresponding $^{206}Pb/^{238}U$ age. Red ellipsoidal spot is approximately 30 × 20 μm. Data shown as gray circles were not used for the age calculations. (For interpretation of the references to color in this figure legend, the reader is referred to the Web version of this article).

Order Podocopida Sars, 1866
Suborder Cypridocopina Baird, 1845
Superfamily Cypridoidea Baird, 1845
Family Cyprideidae Martin, 1940

Genus *Cypridea* Bosquet, 1852
Type species: *Cypris granulosa* Sowerby, 1836

Cypridea tubercularis (Pang in Pang et al., 1984)
Fig. 5A–H; Table 1

1984 *Cypridea* (*Cypridea*) *jiandeensis tubercularis*, Pang et al., p. 121–122, pl. 29, figs. 4–8, pl. 38, figs. 12–13.
1985a *Cypridea* (*Cypridea*) *tubercularis*, Zhang, p. 22–23, pl. 2, figs. 7–10.
1985a *Cypridea* cf. *tubercularis*, Zhang, p. 80, pl. 3, figs. 3a–c.
2002 *Cypridea tubercularis*, Hou et al., p. 428, pl. 164, figs. 9–11.

Material. More than two hundred specimens, mostly complete carapaces with well to moderately preserved.
Dimensions. L: 0.92–1.20 mm; H: 0.68–0.76 mm; W: 0.52–0.68 mm.
Remarks. The studied specimens match the description of subspecies *Cypridea* (*Cypridea*) *jiandeensis tubercularis* Pang, 1984 (in Pang et al., 1984) very well. Zhang (1985a) promoted this subspecies to the species level and stated that variation in shape of species *Cypridea tubercularis* is due to sexual dimorphism, with the more elongate forms representing males. However, after then, Hou et al. (2002) disagree with Zhang's sexual dimorphism hypothesis and considered that the differences of size, size-ratios and shapes of carapaces in *C. tubercularis* indicated the intraspecific variation. In this study, two distinctive adult morphotypes always co-occur in the same samples; one morph with more elongated and less laterally inflated carapace is most likely the male (Fig. 5A–D), another morph with higher width and more laterally inflated carapace indicates the female (Fig. 5E–H). Therefore, we follow Zhang's (1985a) concept, *C. tubercularis* represents sexual dimorphism.
Distribution. Upper part of the Dabeigou Formation (= Dadianzi Formation) of the Luanping Basin (Pang et al., 1984); Yixian Formation of western Liaoning (Zhang, 1985a); Yingzuilazi Formation of the Baishan Basin (this study).

Cypridea horni Wang, sp. nov.
LSID urn: lsid: zoobank.org:act:522441B4-D595-4854-9466-66F9D72A061C.
Fig. 5I–N; Table 1

Derivation of name. Named for Prof. David J. Horne in recognition of his great contribution to our understanding of fossil and living ostracods, and for being a mentor to YQW over many years.
Holotype. NIGP 176376 (Fig. 5I and J), complete adult carapace, sample YZLZ-11 from the Yingzuilazi section of the Yingzuilazi Formation, L: 1.20 mm, H: 0.84 mm, W: 0.72 mm.
Paratype. NIGP 176377 (Fig. 5K and L), complete adult carapace, sample YZLZ-9-1 from the Yingzuilazi section of the Yingzuilazi Formation, L: 1.16 mm, H: 0.72 mm, W: 0.64 mm; NIGP 176378 (Fig. 5M), complete adult carapace, sample YZLZ-9-1 from the Yingzuilazi section of the Yingzuilazi Formation, L: 1.16 mm, H: 0.76 mm, W: 0.64 mm; NIGP 176379 (Fig. 5N), complete adult carapace, sample YZLZ-9-1 from the Yingzuilazi section of the Yingzuilazi Formation, L: 1.24 mm, H: 0.84 mm, W: 0.68 mm.
Type locality. Yingzuilazi section of the Baishan Basin, Yingzuilazi Formation, Jilin, China.
Material. More than one hundred well to moderately preserved carapaces and twenty-three valves.
Dimensions. L: 1.04–1.28 mm; H: 0.72–0.96 mm; W: 0.60–0.76 mm.
Diagnosis. Large to very large sized *Cypridea*, carapace shape approximate triangular to oblong in lateral view, with distinct rostrum, and broader alveolar furrow in LV. Hinge margin incised, forming an extremely visible dorsal furrow; dorsal furrow and outlines of both valves forming a lip-like structure in dorsal view. Carapace surface punctate with presence of tubercles.
Description. Carapace with large to very large in size with approximate triangular to oblong laterally (Fig. 5I–J) and ovate in dorsal and ventral views (Fig. 5M, N). LV > RV, inequivalve, LV overlapping RV along free margin. Maximum height at anterior at or slightly behind mid-length. Maximum length slightly below mid-height, maximum width at mid-length. Anterior margin broad and almost equicurvate with visible short rostrum and broad alveolus. Anterior cardinal angle rounded, somewhat protruding in RV. Posterior margin narrower than anterior one, equicurvate or slightly infracurvate, with posteroventral triangular or slightly rounded cyathus weakly developed in the LV. Posterior cardinal angle strongly rounded. Dorsal margin straight and strongly inclined towards posterior end. Dorsal outline in LV always overtopping in RV, strongly convex in LV and straight in RV. Hinge margin incised, forming an extremely visible dorsal furrow; dorsal furrow and outline forming a lip-like structure in dorsal view (Fig. 5M). Ventral margin straight. Ventral outline slightly concave in RV, and slightly convex in LV. Rostrum well-developed, but not overreaching ventral margin and its point moderately acute. Alveolus relatively well-developed; alveolar notch triangular but distinct and somewhat broad, and alveolar furrow broad extending upwards to 1/5 height of carapace/valve and more visible in LV. Carapace surface finely to moderately punctate but except for dorsal, anterior and posterior margin areas, also characterized by tubercles located close to anterodorsal, posteroventral and posterodorsal parts and arranged in rows in the LV. Moderate variation in ornamentation, presence, number, size and intensity in development of tubercles showing difference in different specimens.
Remarks. The new species strongly resembles *Cypridea* species from the Lower Cretaceous sediments of Mongolia, as described by Galeeva (1955) and Sinitsa (1993); however, *C. unicostata* Galeeva, 1955 has a ventral ridge in LV and lack the lip-like dorsal structure, and *C. elevata* Sinitsa, 1993 is distinctly bigger with alveolar furrow absent. *Cypridea borhuaensis* Gou and Wang, 1986 (in Gou et al., 1986) is similar to *Cypridea horni* sp. nov. in general outline but differs from the latter by its two short node-like ridges in ventral margin area of each valve.
Distribution. Yingzuilazi Formation of the Baishan Basin (this study).

Cypridea bulumensis Sinitsa, 1992
Fig. 6A–F; Table 1

1992 *Cypridea bulumensis*, Sinitsa, p. 23–24, pl. 3, fig. 6.

Material. Sixty well to moderately preserved carapaces and twelve valves.
Dimensions. L: 1.08–1.36 mm; H: 0.40–0.88 mm; W: 0.40–0.64 mm.
Remarks. The specimen studied resembles *Cypridea xiaogushanensis* Zhang, 1985b in general outline and surface ornamentation. The latter shows no distinct alveolar furrow in left valve and with more arched dorsal margin. Moreover, Wang et al. (2013) considered that *C. xiaogushanensis* might be a synonymy of *Cypridea deplecta* Zhang, 1985a.
Distribution. Transbaikalia area of Russia (Sinitsa, 1992); Yingzuilazi Formation of the Baishan Basin.

Cypridea* aff. *multispinosa Hou, 1958

Fig. 6H–R; Table 1

aff. 1958 *Cypridea multispinosa*, Hou, p. 43–44, pl. 2, figs. 8–11.
?1979 *Cypridea multispinosa*, Pang, p. 31–32, pl. 2, figs. 4–8, pl. 7, fig. 8.
1982 *Cypridea multispinosa*, Pang, p. 67, pl. 8, figs. 4–8, pl. 15, fig. 1.
aff. 2002 *Cypridea multispinosa*, Hou et al., p. 404, pl. 148, figs. 4–6.
aff. 2005 *Cypridea multispinosa*, Neustrueva et al., p. 37, pl. 9, figs. 3a–b.

Material. Twenty moderately to badly preserved carapaces and twenty-three badly preserved valves with most of them compressed and covered with sediment fragments.
Dimensions. L: 1.12–1.28 mm; H: 0.72–0.80 mm; W: 0.60–0.76 mm.
Description. Very large sized carapace, outline approximately rounded rectangle to elongated ovate in lateral view to subovate or elliptic in dorsal and ventral views. LV larger than RV, inequivalve, LV overlapping RV along all margins except for dorsal margin. Maximum height slightly behind mid-length or at anterior cardinal angle area. Maximum length at mid-height, maximum width at mid-length. Anterior margin broad and almost equicurvate to somewhat infracurvate. Anterior cardinal angle rounded in LV and somewhat protruding in RV. Posterior margin narrower than anterior one, equicurvate or slightly infracurvate, with posteroventral rounded cyathus which weakly developed in the RV. Posterior cardinal angle strongly rounded. Dorsal margin arched and inclined towards posterior end, developed a ridge-like structure along the dorsal outline in LV. Dorsal outline of LV always overtopping of RV. Hinge margin incised, forming an extremely visible and wide dorsal furrow. Ventral margin straight, ventral outline slightly convex. Rostrum short and broad associated with a wide alveolus, alveolar notch short and small, alveolar furrow broad extending upwards to 1/3 height of carapace/valve in LV, but short in RV. Carapace surface finely to moderately punctate except for dorsal, anterior, and posterior margin areas, also covered by tubercles located close to anterodorsal, posteroventral and posterodorsal areas but showing low density in central part. Moderate variation in ornamentation, presence, number, size, and intensity in development of tubercles showing difference in different specimens. Sexual dimorphism present. Females smaller, more inflation in dorsal and ventral views, and more strongly developed tubercles (Fig. 6H–M); males larger and more elongated in lateral view and less hinge margin inclinations (Fig. 6N–Q). Juvenile individual shows a more remarkable anterior cardinal angle and less degree development of ornamentation (Fig. 6R).
Remarks. Our species show closer affinities to *Cypridea multispinosa* Hou, 1958. The size range of our adult specimens is smaller than in *C. multispinosa* of Hou (1958), Hou et al. (2002) and Neustrueva et al. (2005). The development of alveolar furrow in LV seems to be wider and more visible in our specimens than in *C. multispinosa*, as well as the distribution patterns of tubercles and spines of both are different. *C. multispinosa* of Pang (1979) may belong to *Cypride*a aff. *multispinosa* Hou, 1958 based on Pang (1979)'s description such as elongated ovate carapace shape and developed a ridge-like structure along the dorsal outline. However, his illustrations are of poor quality, for more details, we need to check the original collection material. Therefore, it is given a question mark. *C. multispinosa* from the Lisangou and Guyang formations (Pang, 1982) show striking similarities to our specimens in lateral outline, and the carapace/valve surface characters, as well as shape of the rostrum.
Distribution. *C. multispinosa* was reported from the Lower Cretaceous sediments from Shanxi Province of China (Hou, 1958) and Tsagaantsav Formation (?) of Mongolia (Neustrueva et al., 2005). *C.* aff. *multispinosa* is found in the Lisangou and Guyang formations (Pang, 1982) and the Yingzuilazi Formation of the Baishan Basin.

Cypridea* cf. *unicostata Galeeva, 1955
Fig. 7A–D; Table 1

1955 *Cypridea unicostata*, Galeeva, p. 34–35, pl. 4, fig. 2.
1985a *Cypridea unicostata*, Zhang, pl. 10, figs. 7a–c.
1986 *Cypridea unicostata*, Gou et al., p. 50–51, pl. 12, figs. 7–9.
2002 *Cypridea unicostata*, Hou et al., p. 452, pl. 166, figs. 20–21.

Material. Twenty carapaces and twenty-one valves with filled sediments. L: 1.00–1.20 mm; H: 0.64–0.76 mm; W: 0.52–0.60 mm.
Remarks. Our species share diagnostic features of *C. unicostata* of Galeeva (1955), Zhang (1985a), Gou et al. (1986) and Hou et al. (2002): A approximately trapezoidal carapace in lateral view; a visible alveolar furrow in each valve; a deep dorsal furrow; and surface with punctations and small tubercles; however, our specimens develop less degree of ventral ridge or almost absent ventral ridge. Thus, our specimens are attributed to *C.* cf. *unicostata*.
Distribution. *Cypridea unicostata* has been described from the Lower Cretaceous sediments of Mongolia (Galeeva, 1955), the Jiufotang, Saihantala, Xiguayuan, Guantou, Fengtai, Dahuichang, and Lianmuqin formations of China (e.g. Zhang, 1985a; Gou et al., 1986; Hou et al., 2002).

Cypridea beipiaoensis (Cao, 1999)
Fig. 7E–I; Table 1

1999 *Cypridea* (*Ulwellia*) *beipiaoensis*, Cao, p. 136, pl. 3, figs. 1–13.
2017 *Cypridea beipiaoensis*, Wang et al., p. 346–347, figs. 6A–G.

Material. More than one hundred well to moderately preserved carapaces and thirty valves.
Dimensions. L: 1.08–1.20 mm; H: 0.64–0.84 mm; W: 0.56–0.64 mm.
Remarks. The studied specimens match perfectly with the emended diagnosis and description of *Cypridea beipiaoensis* (Cao, 1999) in Wang et al. (2017), such as RV larger than LV, developing of a remarkable anterior cardinal angle and the distribution pattern of tubercles. Wang et al. (2017) stated that the *C. beipiaoensis* strongly resemble *C. justa* of Lübimova (1956), and the latter one may represent the juvenile stage of the former one. For further confirmation, the original material as well as topotypes of *C. justa* is required.
Distribution. Yixian Formation of western Liaoning (Cao, 1999; Wang et al., 2017); Yingzuilazi Formation of the Baishan Basin (this study).

Family Ilyocyprididae Kaufmann, 1900

Genus *Rhinocypris* Anderson, 1941
Type species: *Rhinocypris scabra* Anderson, 1941

Rhinocypris jurassica (Martin, 1940)
Fig. 8A–D; Table 1

1940 *Ilyocypris jurassica jurassica*, Martin, p. 313, pl. 4, figs. 51–54.
1940 *Ilyocypris jurassica spinosa*, Martin, p. 316, pl. 4, figs. 55–57.
2002 *Rhinocypris jurassica*, Hou et al., p. 391, pl. 144, figs. 1–2, 9–10.
2016 *Rhinocypris jurassica*, Wang et al., p. 412–413, figs. 4P–R.

Material. Twelve moderately to badly preserved carapaces and seven valves.
Dimensions. L: 0.64–0.84 mm; H: 0.36–0.44 mm; W: 0.32–0.40 mm.
Remarks. Although the carapace surfaces of our specimens are dissolved, the studied specimens can assign to species *R. jurassica* by general outline, dimension, and the presence of a visible groove

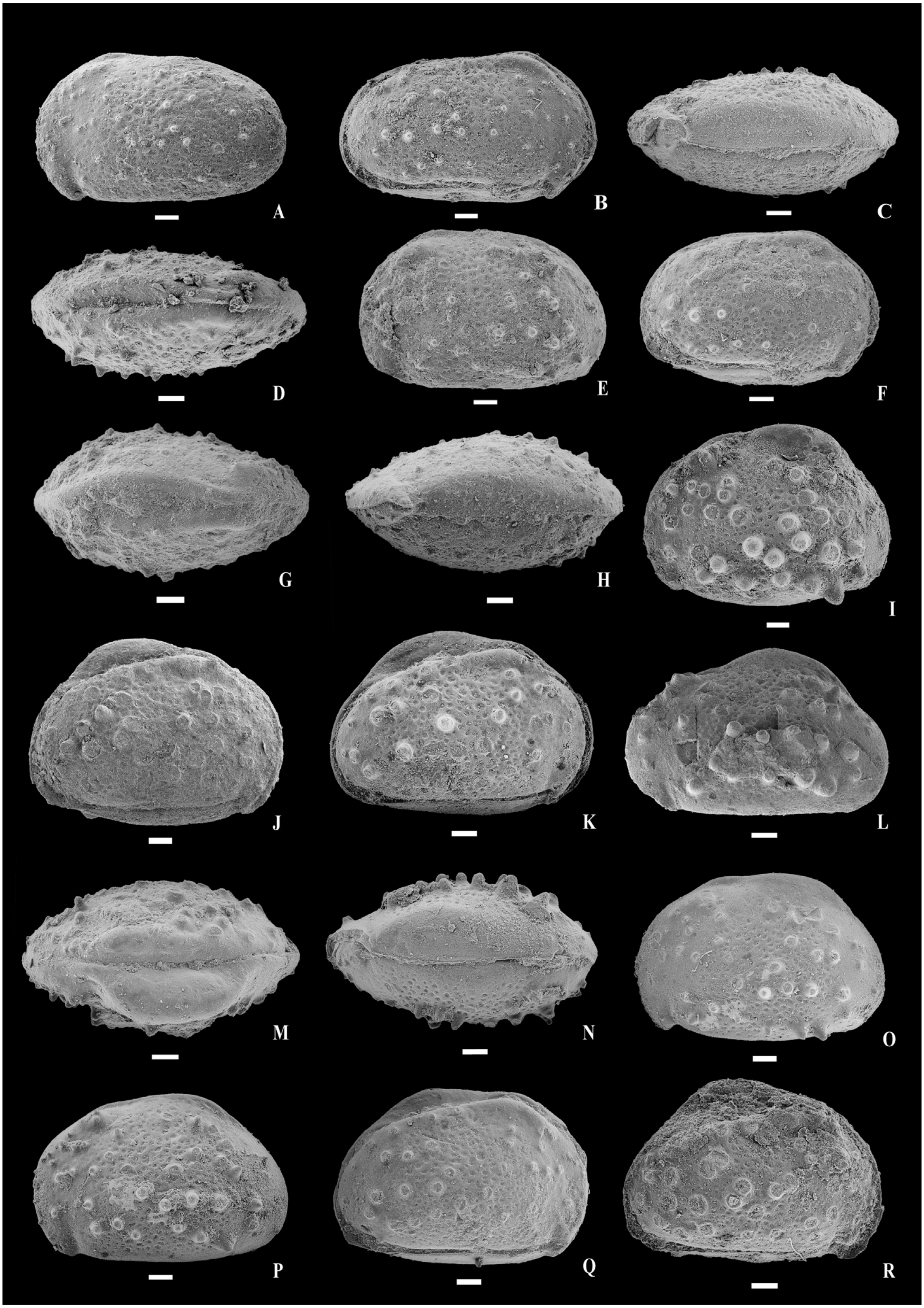

Fig. 5. A–H. ***Cypridea tubercularis*** (Pang in Pang et al., 1984), A, left view of male adult carapace, NIGP 176368, sample YZLZ-4, B, right view of male adult carapace, NIGP 176369, sample YZLZ-4, C, ventral view of male adult carapace, NIGP 176370, sample YZLZ-7-2, D, dorsal view of male adult carapace, NIGP 176371, sample YZLZ-4, E, left view of female adult carapace, NIGP 176372, sample YZLZ-7-1, F, right view of female adult carapace, NIGP 176373, sample YZLZ-7-1, G, dorsal view of female adult carapace, NIGP 176374, sample YZLZ-7-1, H, ventral view of female adult carapace, NIGP 176375, sample YZLZ-7-1; I–R. ***Cypridea horni* sp. nov.** Wang, I, left view of adult carapace, NIGP 176376, sample YZLZ-11, J, right view of adult carapace, NIGP 176376, sample YZLZ-11; K, right view of adult carapace, NIGP 176377, sample YZLZ-9-1, L, left view of adult carapace, NIGP 176377, sample YZLZ-9-1, M, dorsal view of adult carapace, NIGP 176378, sample YZLZ-9-1, N, ventral view of adult carapace, NIGP 176379, sample YZLZ-9-1, O, left view of adult carapace, NIGP 176380, sample YZLZ-9-1, P, left view of adult carapace, NIGP 176381, sample YZLZ-9-1, Q, right view of adult carapace, NIGP 176382, sample YZLZ-9-1, R, right view of adult carapace, NIGP 176383, sample YZLZ-11. Scale bar is 100 μm.

Table 1
Distribution and occurrence of ostracod species in the Yingzuilazi Formation at the Yingzuilazi section of the Baishan Basin.

FORMATION	Yingzuilazi Formation												
SAMPLE ID	YZLZ-4	YZLZ-7	YZLZ-7-1	YZLZ-7-2	YZLZ-8-1	YZLZ-8-2	YZLZ-9-1	YZLZ-11	YZLZ-12	YZLZ-12-1	YZLZ-16	YZLZ-17	YZLZ-17-1
Cypridea tubercularis	Abundant	Few	Abundant	Abundant		Few	Few						
Cypridea horni sp. nov.					Few	Few	Abundant	Abundant	Common				
Cypridea bulumensis									Common	Abundant	Few	Few	
Cypridea aff. *multispinosa*									Common	Few			
Cypridea cf. *unicostata*						Few	Common	Common					
Cypridea beipiaoensis													Abundant
Rhinocypris jurassica													Common
Rhinocypris sp.													Few
Djungarica sp.													Few
Ziziphocypris linchengensis													Abundant
Lycopterocypris infantilis						Few	Few						Few
Lycopterocypris delilis								Few			Few		Few
Timiriasevia principalis													Few
Alicenula? dadianziensis							Few						Few
Alicenula? leguminella	Few		Few				Few						

Few — Common — Abundant

and two nodes. Wang et al. (2016) concluded this species is worldwide distribution species.
Distribution. Upper Purbeck or basal Wealden, UK (Anderson, 1985); Campolara Formation, Spain (Schudack and Schudack, 2012); Yixian, Puchanghe, Shouchang, Lianmuxin, Xiwa and Saihantala formations of China (Hou et al., 2002; Wang et al., 2016), Yingzuilazi Formation of the Baishan Basin (this study).

***Rhinocypris* sp.**
Fig. 8E; Table 1

Material. Only one valve, L: 0.68 mm; H: 0.32 mm; W: ?
Remarks. The presence of three nodes, two depression and the thin shell place the studied specimens within the Genus *Rhinocypris*. This single specimen may represent a new species, however, with only one left valve collected, the material is not sufficient to propose a new species.
Distribution. Yingzuilazi Formation of the Baishan Basin (this study).

Family Djungarididae Gou and Hou, 2002 (in Hou et al., 2002)

Genus *Djungarica* Galeeva, 1977 (in Ye et al., 1977)
Type species: *Djungarica saidovi* Galeeva, 1963 in Nanjing Institute of Geology and Palaeontology, Chinese Academy of Sciences (1963)

***Djungarica* sp.**
Fig. 8F; Table 1

Material. Three carapaces and one broken valve, L: 1.92–2.04 mm; H: 1.24–1.36 mm; W: 0.92–1.08 mm.
Remarks. The specimens available are poorly preserved and many details are not visible, but the gigantic size and approximately triangular lateral carapace outline fit emended diagnostic of the Genus *Djungarica* in Hou et al. (2002). The carapace shape of our specimens is quite similar with *D. circulitriangula* Zhang, 1985a (see Zhang, 1985a, pl. 21 figs. 4a-c), but our specimen is distinctly bigger. This species is similar to *Mantelliana chanhilensis* Sinitsa, 1973 in general outline. The problem is that in Sinitsa (1973), no diagnosis and description are given for her new species *M. chanhilensis* and her illustrations are of poor quality. Thus, we need to check the original material for further confirmation.
Distribution. Yingzuilazi Formation of the Baishan Basin (this study).

Family Ziziphocyprididae Chen, 2002 (in Hou et al., 2002)

Genus *Ziziphocypris* Chen, 1965
Type species: *Timiriasevia costata* Galeeva, 1955

***Ziziphocypris linchengensis* Su and Li, 1981**
Fig. 8G–L, Table 1

1981 *Ziziphocypris linchengensis*, Su and Li, p. 124, pl.2, figs. 1–17.
1992 *Ziziphocypris galeevae*, Sinitsa, p. 28, pl. 4, fig. 1.
2002 *Ziziphocypris linchengensis*, Hou et al., p. 690, pl. 296, figs. 11–16.
2016 *Ziziphocypris linchengensis*, Wang et al., p. 416, figs. 6A–F.

Material. More than hundred well to moderately preserved carapaces and forty valves, L: 0.60–0.76 mm; H: 0.44–0.56 mm; W: 0.28–0.44 mm.
Remarks. The studied specimens assign to *Ziziphocypris linchengensis* Su and Li, 1981 in general outline, surface ribs ornamentation and two visible dorsal ridges in each valve. The synonym

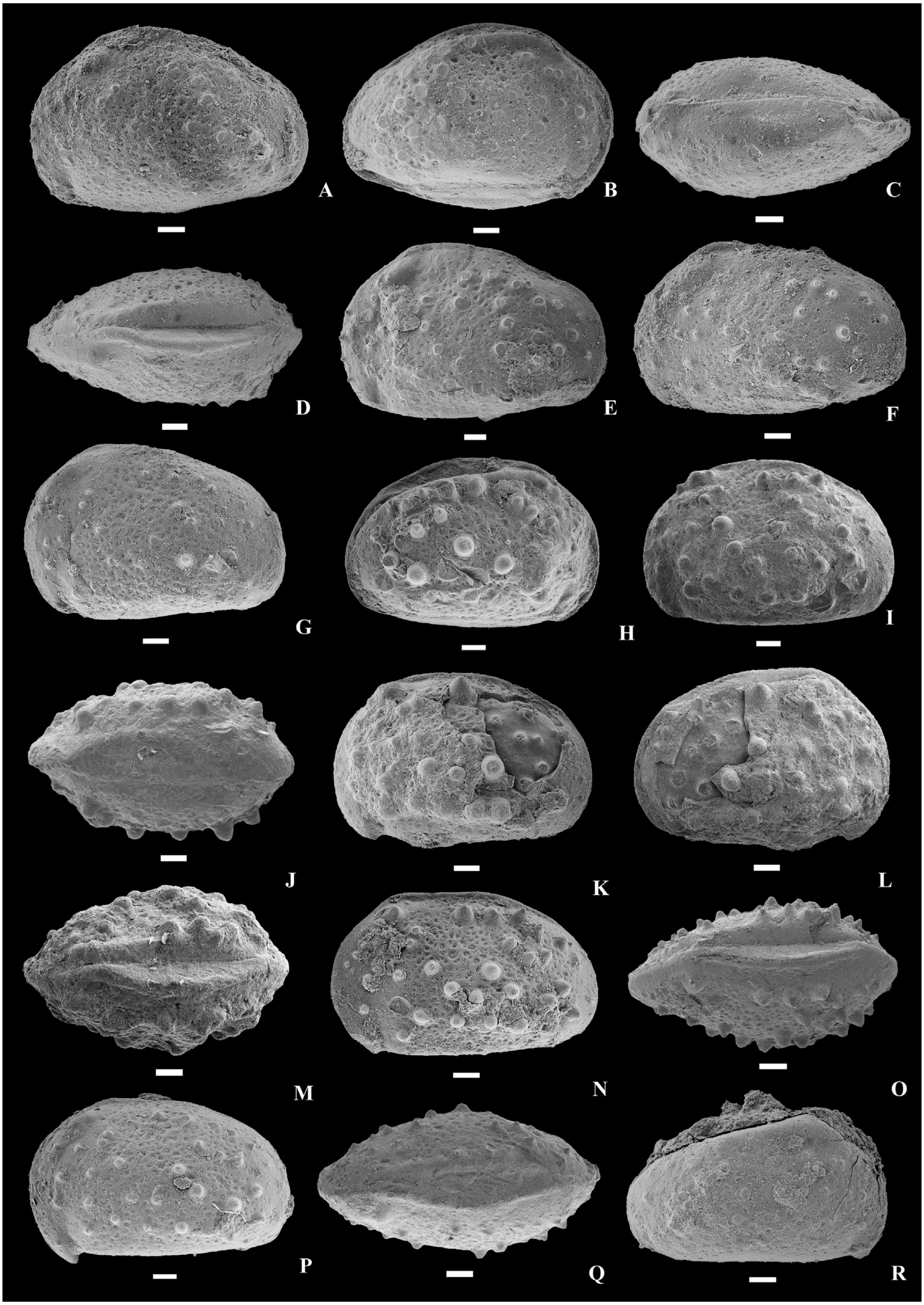

Fig. 6. A–G. ***Cypridea bulumensis*** Sinitsa, 1992, A, left view of adult carapace, NIGP 176384, sample YZLZ-12-1, B, right view of adult carapace, NIGP 176385, sample YZLZ-12-1, C, ventral view of adult carapace, NIGP 176386, sample YZLZ-12-1, D, dorsal view of adult carapace, NIGP 176387, sample YZLZ-12-1, E, left view of adult carapace, NIGP 176388, sample YZLZ-16, F, left view of adult carapace, NIGP 176389, sample YZLZ-17, G, left view of adult carapace, NIGP 176390, sample YZLZ-12; H–R. ***Cypridea* aff. *multispinosa*** Hou, 1958, H, right view of female carapace, NIGP 176391, sample YZLZ-12, I, left view of female carapace, NIGP 176391, sample YZLZ-12, J, ventral view of female carapace, NIGP 176391, sample YZLZ-12, K, left view of female carapace, right view of female carapace, NIGP 176392, sample YZLZ-12-1, L, right view of female carapace, NIGP 176392, sample YZLZ-12-1, M, dorsal view of male carapace, NIGP 176393, sample YZLZ-12, N, left view of male carapace, NIGP 176394, sample YZLZ-12, O, dorsal view of male carapace, NIGP 176394, sample YZLZ-12, P, left view of male carapace, NIGP 176395, sample YZLZ-12, Q, dorsal view of male carapace, NIGP 176395, sample YZLZ-12, R, lateral view of juvenile right valve, NIGP 176396, sample YZLZ-12-1. Scale bar is 100 μm.

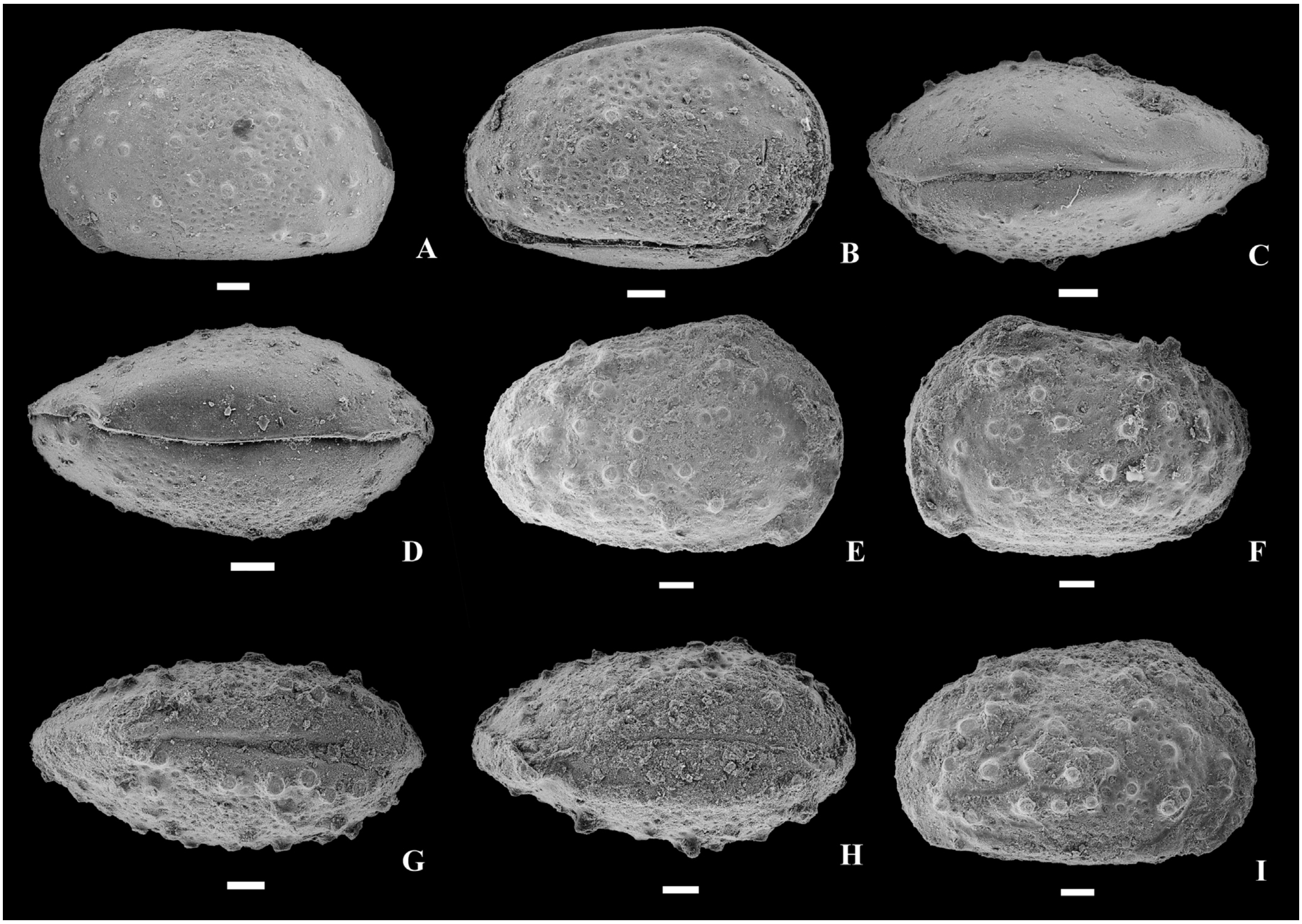

Fig. 7. A–D. ***Cypridea* cf. *unicostata*** Galeeva, 1955, A, left view of adult carapace, NIGP 176397, sample YZLZ-9-1, B, right view of adult carapace, NIGP 176398, sample YZLZ-9-1, C, dorsal view of adult carapace, NIGP 176399, sample YZLZ-9-1, D, ventral view of adult carapace, NIGP 176400, sample YZLZ-9-1; E–D. ***Cypridea beipiaoensis*** (Cao, 1999), E, right view of adult carapace, NIGP 176401, sample YZLZ-17-1; F, left view of adult carapace, NIGP 176402, sample YZLZ-17-1; G, dorsal view of adult carapace, NIGP 176403, sample YZLZ-17-1, H, ventral view of adult carapace, NIGP 176404, sample YZLZ-17-1, I, right view of adult carapace, NIGP 176405, sample YZLZ-17-1. Scale bar is 100 μm.

list in Wang et al. (2016) had included published specimens in Eastern Asia. *Ziziphocypris galeevae* Sinitsa, 1992 is considered a synonym of *Z. linchengensis*, because of sharing the same diagnostic features with specimens of *Z. linchengensis* in Su and Li (1981).
Distribution. Lincheng Formation (Su and Li, 1981), upper part of the Dabeigou Formation (= Dadianzi) Formation of the Luanping Basin (Pang, 1982); Yixian Formation of western Liaoning (Wang et al., 2016); Lisangou Formation (Pang, 1978, 1979); Duhongmu Formation (Li, 1989) and second member of the Saihantala Formation (Gou et al., 1986) of Inner Mongolia; Transbaikalia area of Russia (Sinitsa, 1992).

Family Cyprididae Baird, 1845

Genus *Lycopterocypris* Mandelstam (in Lübimova, 1956)
Type species: *Cypris faba* Egger, 1910

Lycopterocypris infantilis Lübimova, 1956
Fig. 8M–N; Table 1

1956 *Lycopterocypris infantilis*, Lübimova, p. 106, pl. 21, figs.1a–b, 2a, 3a–b.
2016 *Lycopterocypris infantilis*, Wang et al., p. 414–415, figs. 5F–G.

Material. Fourteen moderately to badly preserved carapaces and three valves, L: 0.56–0.68 mm; H: 0.28–0.36 mm; W: 0.16–0.28 mm.
Remarks. The small size and rounded oblong shape of carapace allow our specimens to be identified as *Lycopterocypris infantilis* Lübimova, 1956. The taxonomy, distribution and stratigraphic range of this species had been well discussed by Wang et al. (2016), and their work is followed here.
Distribution. Lisangou, Guyang, Dabeigou, Penglaizheng, Hekou, Dahuichang, Xiazhuang, Fengtai, Yixian, Jiufotang, Fuxin, and Sunjiawan formations, Zhidan Group and Xinmingbao Group of China (e.g. Zhang, 1985a; Hou et al., 2002); Zuunbayan Formation of Mongolia (Lübimova, 1956); Yingzuilai Formation of the Baishan Basin (this study).

Lycopterocypris debilis Lübimova, 1956
Fig. 8O–R; Table 1

1956 *Lycopterocypris debilis*, Lübimova, p. 107, pl. 21, figs. 5a–c.
1985a *Lycopterocypris liaoxiensis*, Zhang, pl. 23, figs. 3a–c, 4a–c.
1985b *Lycopterocypris liaoxiensis*, Zhang, p. 145, pl. 3, figs. 7a–c.
2016 *Lycopterocypris debilis*, Wang et al., p. 415, figs. 5H–I.

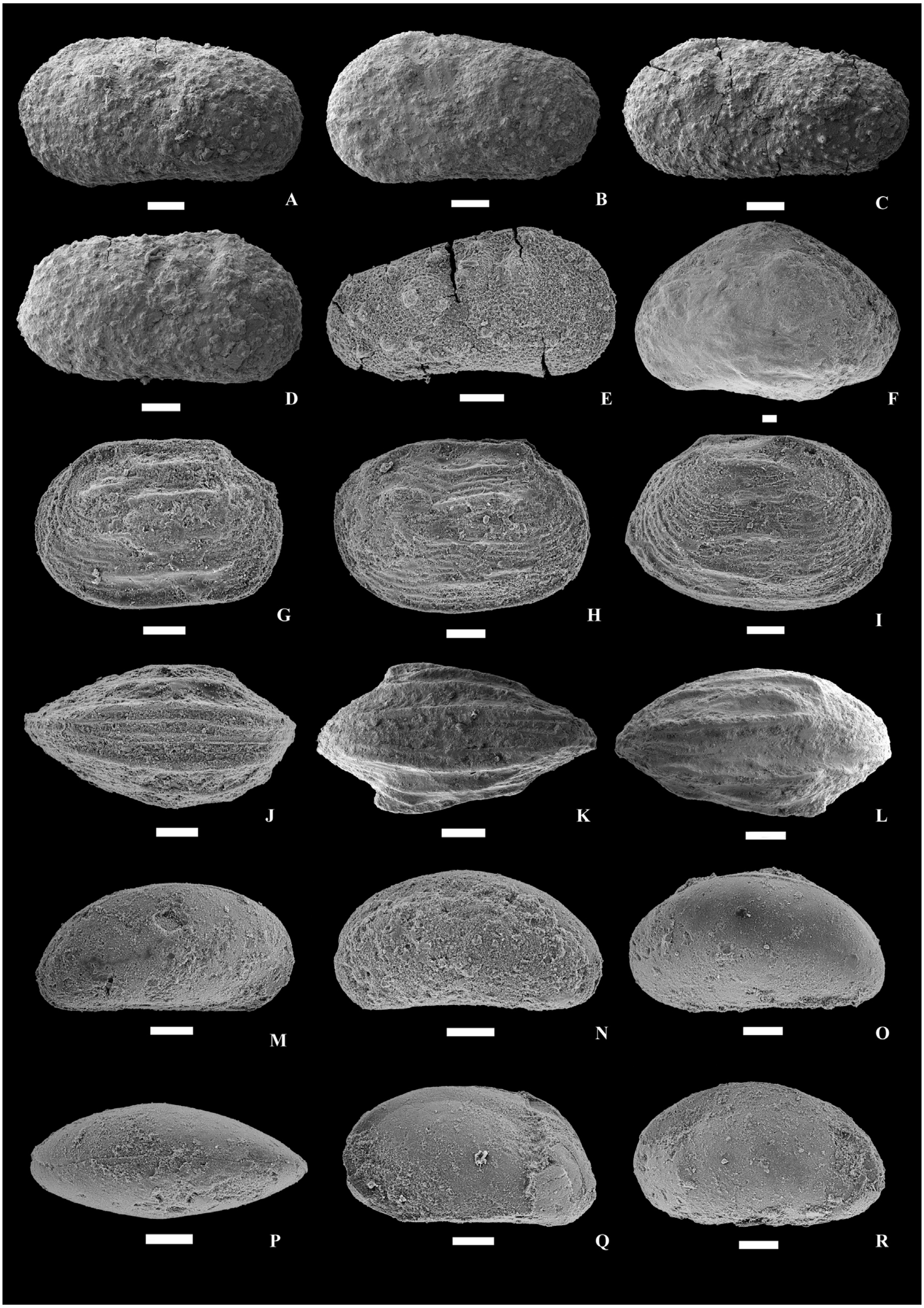

Fig. 8. A–D. ***Rhinocypris jurassica*** (Martin, 1940), A, left view, NIGP 176406, sample YZLZ-17-1, B, left view, NIGP 176407, sample YZLZ-17-1, C, left view, NIGP 176408, sample YZLZ-17-1, D, right view, NIGP 176409, sample YZLZ-17-1; E. ***Rhinocypris* sp.**, lateral view of right valve, NIGP 176410, sample YZLZ-17-1; F, ***Djungarica* sp.**, left view of carapace, NIGP 176411, sample YZLZ-17-1; G–L. ***Ziziphocypris linchengensis*** Su and Li, 1981, A, left view of, NIGP 176412, sample YZLZ-17-1, B, left view of, NIGP 176413, sample YZLZ-17-1, I, right view of, NIGP 176414, sample YZLZ-17-1, J, ventral view of, NIGP 176415, sample YZLZ-17-1, K, ventral view of, NIGP 176416, sample YZLZ-17-1, L, dorsal view of carapace, NIGP 176417, sample YZLZ-17-1; M–N. ***Lycopterocypris infantilis*** Lübimova, 1956, M, right view of carapace, NIGP 176418, sample YZLZ-9-1, N, left view of carapace, NIGP 176419, sample YZLZ-17-1; O–R. ***Lycopterocypris debilis*** Lübimova, 1956, O, left view of carapace, NIGP 176420, sample YZLZ-9-1, P, dorsal view of carapace, NIGP 176421, sample YZLZ-9-1, Q, left view of broken carapace, NIGP 176422, sample YZLZ-9-1, R, left view of compressed carapace, NIGP 176423, sample YZLZ-9-1. Scale bar is 100 μm.

Material. Twenty moderately to badly preserved carapaces and five valves, L: 0.60–0.68 mm; H: 0.32–0.40 mm; W: 0.20–0.24 mm.
Remarks. The size, overlap and carapace outlines in lateral and dorsal view all allow the studied specimens to be identified as *Lycopterocypris debilis* Lübimova, 1956. We agree with the emended diagnostic features of species *L. debilis* by Wang et al. (2016).
Distribution. Guyang and Jiufotang formations, Xinmingbao Group (Wang et al., 2016); Zuunbayan Formation in Mongolia (Lübimova, 1956); Yingzuilai Formation of the Baishan Basin (this study).

Superfamily Cytheroidea Baird, 1845
Family Limnocytheridae Sars, 1928
Subfamily Timiriaseviinae Mandelstam, 1960

Genus *Timiriasevia* Mandelstam, 1947
Type species: *Timiriasevia epidermiformis* Mandelstam,1947

Timiriasevia principalis Lübimova, 1956
Fig. 9A–C; Table 1

1956 *Timiriasevia principalis*, Lübimova, p. 129–130, pl. 24, figs. 1a–b.
1965 *Metacypris miaogouensis*, Chen, p. 19–20, pl. 1, figs. 10–13.
? 2004 *Timiriasevia principalis*, Van Itterbeeck et al., p. 403, figs. 4N–O.
2005 *Timiriasevia principalis*, Neustrueva et al., pl. 27, figs. 7–8.

Material. Six moderately to badly preserved carapaces and three valves with two broken, L: 0.48–0.72 mm; H: 0.28–0.44 mm; W: 0.32–0.44 mm.
Remarks. Although the studied specimens with incomplete valves and carapaces covered with sediments, the general outline of valve and the distinct ornamentation allow the attribution of the specimens to the species *Timiriasevia principalis* Lübimova, 1956. Van Itterbeeck et al. (2004) stated that the species *Metacypris miaogouensis* Chen, 1965 is a junior synonym of *T. principalis*, which is followed in this study. However, the specimens of *T. principalis* in Van Itterbeeck et al. (2004) may not belong to this species even the Genus *Timiriasevia*. The figured incomplete specimens of Van Itterbeeck et al. (2004) strongly resemble species *Paracypretta dashuigouensis* Huang, 1985 (probably belongs to the Genus *Zonocypris*; for further confirmation, we need to examine the original material) in lateral valve outline and the fingerprint-like surface ornamentation (see Van Itterbeeck et al., 2004, figs. 4N–O and Huang, 1985, pl. 2, figs. 17–18), which are both from the Dashuigou Formation of Inner Mongolia. Compared with the representative of the Genus *Timiriasevia*, the *P. dashuigouensis* specimen of Huang (1985) (see Huang, 1985, pl. 2, figs. 17–18) shows more inflated carapace outline in dorsal view and lacks the antero-lateral constriction as well as covered with fingerprint-like ornamentation. Therefore, the synonymy of *T. principalis* in Van Itterbeeck et al. (2004) is given a question mark here.
Distribution. Sainshand suite of Mongolia (Lübimova, 1956; Neustrueva et al., 2005); Cretaceous strata (Miaogou) of Gansu Province (Chen, 1965); upper part of the Dabeigou Formation (= Dadianzi Formation); Yingzuilazi Formation of the Baishan Basin (this study).

Superfamily Darwinuloidea Brady and Norman, 1889
Family Darwinulidae Brady and Norman, 1889

Genus *Alicenula* Rossetti and Martens, 1998
Type species: *Darwinula serricaudata* Klie, 1935

Remarks. Although Martens et al. (2003) assigned some fossil darwinuloidean specimens from England Purbeck sediments to the extant Genus *Alicenula* based on valves internal structures and the carapace overlap. However, the assignment of fossil darwinuloidean species to recent genera remains problematic for reasons, particularly when the internal features are unknown (Antonietto et al., 2018; Trabelsi et al., 2020). Furthermore, no attempts have been carried out to integrate taxonomic approaches for fossil and living darwinuliodean species so far (Antonietto et al., 2018). To address this problem, more detailed taxonomic work and a wide morphological analysis of key specimens from the Superfamily Darwinuloidea are required, however, is out of our topic of present work. Therefore, we tentatively assign our normal carapace overlap species to the Genus *Alicenula* of this study.

Alicenula? dadianziensis (Pang in Pang et al., 1984)
Fig. 9D–I; Table 10.5

1984 *Darwinula dadianziensis*, Pang et al., p. 195–196, pl. 36, fig. 7.

Material. Seven moderately to well preserved carapaces and one broken valve, L: 0.72–0.88 mm; H: 0.40–0.44 mm; W: 0.36–0.40 mm.
Remarks. The general carapace outline and the smooth surface clearly place the studied specimens within *Alicenula*? *dadianziensis* (which is equivalent to *Darwinula dadianziensis* of Pang et al., 1984). This species is similar to *Darwinula darbiensis* Neustrueva (in Neustrueva et al., 2005), but the former one has more inflation posterolateral carapace and more concave ventral margin.
Distribution. Upper part of the Dabeigou Formation (= Dadianzi Formation) of Luanping Basin (Pang et al., 1984 and YQW's unpublished material); Yingzuilazi Formation of the Baishan Basin (this study).

Alicenula? leguminella (Forbes, 1855)
Fig. 9J–R; Table 1

1855 *Cypris leguminella*, Forbes, p. 294, fig. 334c.
2002 *Darwinula leguminella*, Hou et al., p. 751, pl. 303, figs. 5–12.
2003 *Alicenula leguminella*, Martens et al., fig. 3a–u.
2016 *Alicenula leguminella*, Wang et al., p. 419–410, figs. 6M–R.

Material. Ten moderately to well preserved carapaces, L: 0.48–0.68 mm; H: 0.28–0.32 mm; W: 0.24–0.28 mm.
Remarks. The size and shape of the carapace, with the LV overlapping RV on all margins, refers the present specimens to *A. leguminella*, although this species belongs to Genus *Alicenula* is questionable here. We follow the synonym list in Wang et al. (2016).
Distribution. Jinxin, Puchanghe, Jianmenguan, Suining, Zhuanqiao, Shouchang, Guantou, Xiwa, Dabeigou, Zhoujiadian, Yixian and Saihantala formations of China (Hou et al., 2002; Wang et al., 2016); Lulworth Formation, UK; Purbeck/Wealden-like deposits of Germany, Poland, and France; Jydegaard Formation of Denmark; Morrison Formation of USA (Martens et al., 2003); Zuunbayan Formation of Mongolia (Lübimova, 1956); core samples from Araripe and Jatobá basins of Brazil (Tomé et al., 2014).

5. Discussion

5.1. Chronostratigraphy for the Yingzuilazi Formation

The age of Yingzuilazi Formation is poorly constrained because of lacking the radiometric age data. The age of Yingzuilazi Formation was formerly assumed by bracketing ages between the underlying Guosong Formation and overlying Linzitou Formation from the Baishan Basin or adjacent areas (e.g. Pei, 2005; Li, 2006; Li et al., 2011; Chen et al., 2016; Huang, 2016; Guo et al., 2018). The published dates for the Lizitou, Yingzuilazi, and Guosong formations are summarized in Table 2 and briefly discussed as follows. Pei (2005) reported $^{40}Ar/^{39}Ar$ age of 130.2 ± 0.3 Ma for andesite collected from the Guosong Formation of the Hunjiang area. Similar

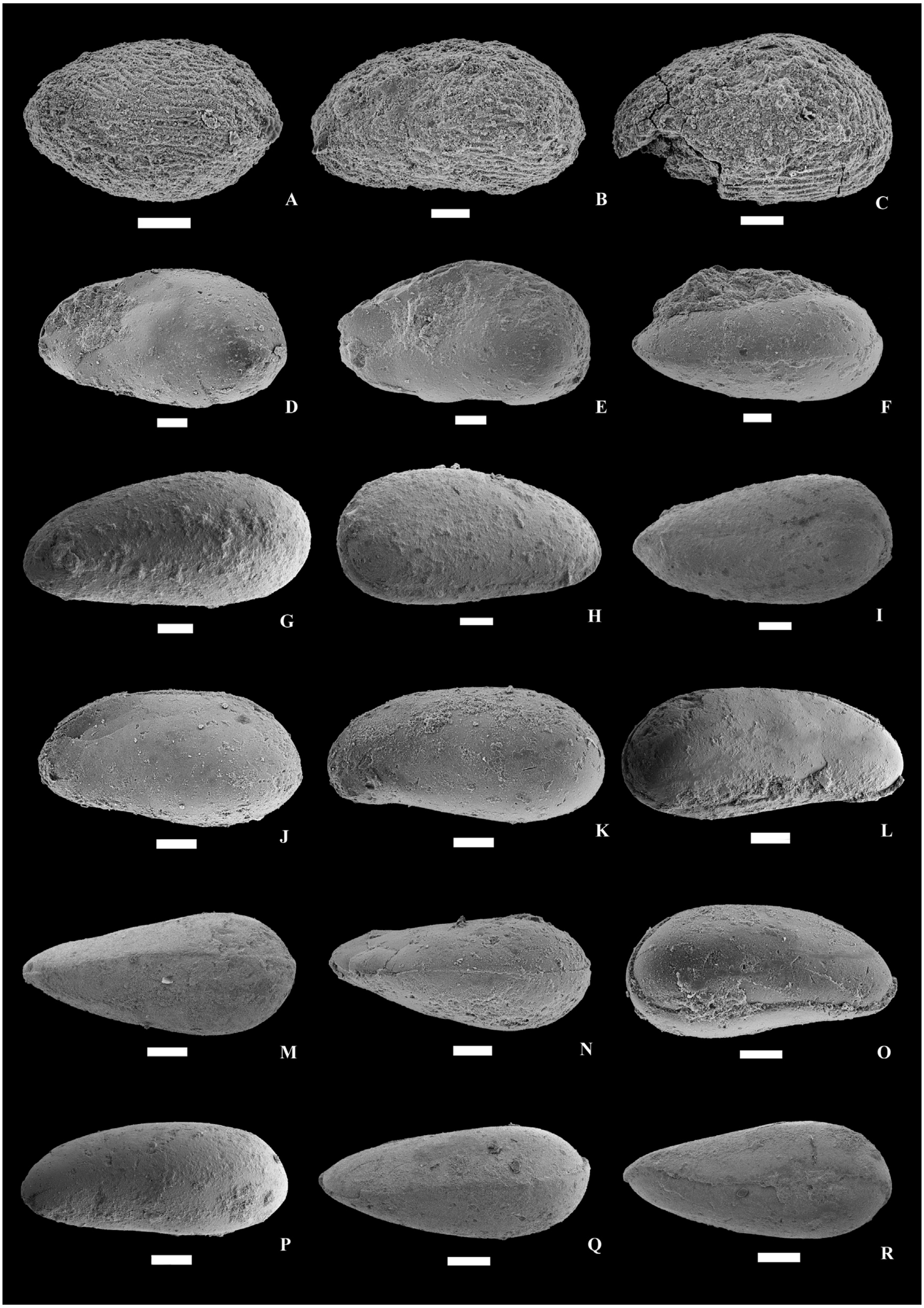

Fig. 9. A–C. ***Timiriasevia principalis*** Lübimova, 1956, A, dorsal view of male carapace, NIGP 176424, sample YZLZ-17-1, B, lateral view of left valve, NIGP 176425, sample YZLZ-17-1, C, lateral view of left view with anterior-ventral part missing, NIGP 176426, sample YZLZ-17-1; D–I. ***Alicenula? dadianziensis*** (Pang in Pang et al., 1984), D, left view of compressed carapace, NIGP 176427, sample YZLZ-7-1, E, left view of compressed carapace, NIGP 176428, sample YZLZ-7-1, F, dorsal view of carapace with sediments, NIGP 176429, sample YZLZ-7-1, G, left view of carapace, NIGP 176430, sample YZLZ-7-1, H, right view of carapace, NIGP 176430, sample YZLZ-7-1, I, ventral view of carapace, NIGP 176430, sample YZLZ-7-1; J–I. ***Alicenula? leguminella*** (Forbes, 1855), J, left view of compressed carapace, NIGP 176431, sample YZLZ-9-1, K, left view of carapace, NIGP 176432, sample YZLZ-9-1, L, right view of carapace, NIGP 176432, sample YZLZ-9-1, M, dorsal view of carapace, NIGP 176432, sample YZLZ-9-1, N, dorsal view of carapace, NIGP 176433, sample YZLZ-9-1, O, right view of carapace, NIGP 176434, sample YZLZ-9-1, P, left view of carapace, NIGP 176434, sample YZLZ-9-1, Q, dorsal view of carapace, NIGP 176434, sample YZLZ-9-1, R, ventral view of carapace, NIGP 176434, sample YZLZ-9-1. Scale bar is 100 μm.

Table 2
Summary of literature age dates of the Lizitou, Yingzuilazi, and Guosong formations from Baishan and adjacent areas.

Formation	Location	Type	Sample No.	Method	Age (Ma)	Reference
Lizitou Fm.	Tonghua–Baishan	andesite	LZT2	LA-ICP-MS U–Pb	126.0 ± 2.9 (n = 5)	Zhao (2015)
	Tonghua–Baishan	andesitic tuff	LZT1	LA-ICP-MS U–Pb	123.2 ± 0.9 (n = 21)	Zhao (2015)
	Tonghua–Baishan	Rhyolitic ignimbrite	LZT3	LA-ICP-MS U–Pb	121–129	Zhao (2015)
	Tonghua	Trachyandesite	20TH-34	Ar–Ar	119.0 ± 0.6	Li (2006)
	Tonghua	trachyte	20TH-46	Ar–Ar	114.0 ± 0.6	Li (2006)
Yingzuilazi Fm.	Liuhe Basin	sandstone	P14-B3	LA-ICP-MS U–Pb	~131	Lan (2019)
	Liuhe Basin	sandstone	L1-B178	LA-ICP-MS U–Pb	~126	Lan (2019)
	Yalu River Basin	tuffaceous siltstone	HD1-3	LA-ICP-MS U–Pb	~126	Pang et al. (2018)
	Baishan Basin			palynology	Hauterivian–Barremian	Guo et al. (2018)
Guosong Fm.	Guosong Basin	andesite	GS-1-TWS	LA-ICP-MS U–Pb	130.8 ± 0.8 (n = 24)	Zhao (2015)
	Hunjiang	andesite	TH8-3	Ar–Ar	130.2 ± 0.3	Pei (2005)
	Guosong Basin	andesite	GS04	LA-ICP-MS U–Pb	130 ± 2 (n = 14)	Liu et al. (2018)
	Tonghua Basin	trachyandesite	16PJ10-2	LA-ICP-MS U–Pb	129 ± 1 (n = 9)	Zhou (2021)
	Guosong Basin	trachyte	16PJ1-7	LA-ICP-MS U–Pb	129 ± 1 (n = 15)	Zhou (2021)
	Guosong Basin	andesite	GS07	LA-ICP-MS U–Pb	129 ± 2 (n = 19)	Liu et al. (2018)
	Tonghua	Trachyandesite	20TH-31	Ar–Ar	125.7 ± 0.6	Li (2006)
	Xinbindong Basin	trachyte	18JF21	SIMS U–Pb	124 ± 1 (n = 20)	Feng et al. (2020)
	Guosong Basin	rhyolite	GS-2-TWS	LA-ICP-MS U–Pb	118.5 ± 1.1 (n = 23)	Zhao (2015)

ages for andesite and trachyte from the Guosong Formation of the Guosong Basin were obtained by LA-ICP-MS (129 ± 1 Ma, 129 ± 2 Ma, 130 ± 2 Ma and 130.8 ± 0.8 Ma; Chen et al., 2016; Liu et al., 2018; Zhou, 2021). Chen et al. (2016) reported LA-ICP-MS U–Pb dating results (123.2 ± 0.9 Ma and 126.0 ± 2.9 Ma) for the tuff samples from the Linzitou Formation of the Tonghua area. However, Li (2006) and Li et al. (2011) reported slightly younger $^{40}Ar/^{39}Ar$ ages of 119.0 ± 0.6 Ma and 114.0 ± 0.6 Ma for trachyandesite/trachyte collected from the Linzitou Formation of the Tonghua area. Thus, the age of the Yingzuilazi Formation is roughly constrained from ~130 Ma to ~123 Ma. On the other hand, all the radiometric results of the Yingzuilazi Formation were determined by LA-ICP-MS U–Pb dating on detrital zircons extracted from sandstone samples from nearby Liuhe and Yalu River basins (Fig. 10; Pang et al., 2018; Lan, 2019). The youngest peak age of the sediments constrains the deposition of the Yingzuilazi Formation to ~127.7 Ma (Fig. 10). In this study, the tuff layer collected from the uppermost part of the Yingzuilazi Formation provide a critical opportunity for geochronological study. Hence, the weighted mean SIMS U–Pb age of 128.5 ± 1.0 Ma could represent the age limit of the Yingzuilazi Formation. In addition, our SIMS data is the first robust radiometric age from the Yingzuilazi Formation, which is consistent with the youngest age group by detrital zircon studies mentioned above.

5.2. Ostracod biostratigraphy and age determination for the Yingzuilazi Formation

Ostracoda, a small crustacean arthropod with a calcified bivalved shell (carapace), have excellent fossil records extending back to Ordovician (e.g. Horne, 2005). Because of their small size, high fossilization potential and frequency of occurrence in nonmarine and marine sediments, thus ostracods are undoubtedly a useful biostratigraphical indicator for regional, supraregional and intercontinental biostratigraphic correlations (e.g. Sames, 2011a,b; Sames and Horne, 2012; Wang et al., 2015; Choi et al., 2020). For the Yingzuilazi Formation, 11 ostracod taxa were reported in the literature (Huang, 2016). Finds from this formation were assigned to genera *Cypridea*, *Lycopterocypris*, *Damonella*, *Yumenia* and *Darwinula*, indicating an Early Cretaceous age with no stage information, but were neither described nor figured (Huang, 2016). Li et al. (2018) proposed a *Cypridea-Lycopterocypirs-Darwinula* ostracod assemblage for the Yingzuilazi Formation and stated that the Yingzuilazi Formation can correlate with the Yixian Formation of western Liaoning. Again, no species description or figures are available. Therefore, more detailed taxonomic and biostratigraphic studies of the ostracod fauna from the Yingzuilazi Formation are requested.

In this study, fifteen ostracod species belonging to seven genera including a new species are described and figured: *Cypridea tubercularis* (Pang in Pang et al., 1984), *C. horni* sp. nov., *C. bulumensis* Sinitsa, 1992, *C.* aff. *multispinosa* Hou, 1958, *C.* cf. *unicostata* Galeeva, 1955, *C. beipiaoensis* (Cao, 1999), *Rhinocypris jurassica* (Martin, 1940), *R.* sp., *Djungarica* sp., *Ziziphocypris linchengensis* Su and Li, 1981, *Lycopterocypris infantilis* Lübimova, 1956, *L. debilis* Lübimova, 1956, *Timiriasevia principalis* Lübimova, 1956, *Alicenula*? *dadianziensis* (Pang, 1984 in; Pang et al., 1984), and *Alicenula*? *leguminella* (Forbes, 1855), all from the type section of the Yingzuilazi Formation. This ostracod fauna is dominated by *Cypridea* species as well as shows a high diverse of non-*Cypridea* species. Besides the world-widely distribution species *Rhinocypris jurassica* and *Alicenula*? *leguminella*, the rest of them seem to be endemic to east Asia. In this fauna, *Cypridea tubercularis* has been found in the upper part of the Dabeigou Formation (= Dadianzi Formation) in Luanping Basin (Pang et al., 1984) and in the Yixian Formation of western Liaoning (Zhang, 1985a). The upper part of the Dabeigou Formation is assigned to Hauterivian to Barremian (based on unpublished biostratigraphy data of YQW). Recently, the upper part of the Dabeigou Formation (= Dadianzi Formation) is constrained to 127.8 Ma (Barremian) by Yu et al. (2022a). The Yixian Formation was dated as a Barremian to Aptian based on biostratigraphic dates (e.g., Sha, 2007; Wang et al., 2015), however, this formation has been recently precisely dated as between 125.755 Ma to 124.122 Ma (Aptian) in the Sihetun area (Zhong et al., 2021). *C. bulumensis* is reported from the Late Jurassic to Early Cretaceous sediments in Transbaikalia area of Russia (Sinitsa, 1992). *C. beipiaoensis* is also found in Yixian Formation of western Liaoning (Cao, 1999; Wang et al., 2017). *Ziziphocypris linchengensis* has been discovered from the Hautervian to Aptian sediments of northeast China and eastern Mongolia, and from Early Cretaceous in Transbaikalia area of Russia (e.g. Su and Li, 1981; Pang, 1982; Sinitsa, 1992; Xin et al., 2000; Wang et al., 2016). The distributions of species *Lycopterocypris infantilis* and *L. debilis* have been well documented and summarized in Wang et al. (2016), these two species are widely distributed in Hauterivian to Albian non-marine strata of east Asia (Wang et al., 2016 and see reference therein). *Timiriasevia principalis* was reported from the Dabeigou Formation in the Luanping Basin and the Sainshand suite of Mongolia (Lübimova, 1956; Neustrueva et al.,

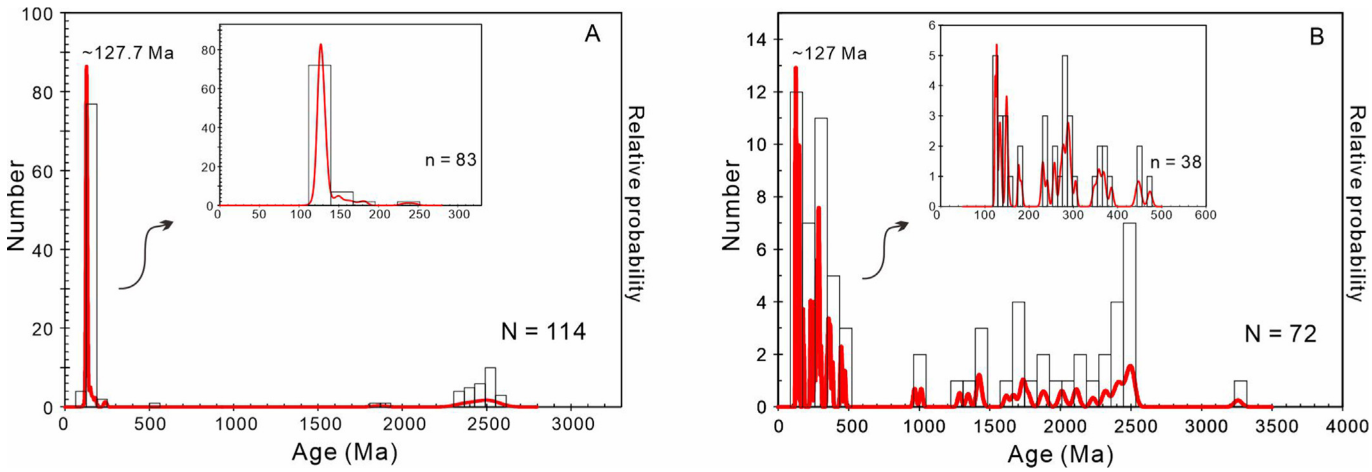

Fig. 10. Histograms of LA-ICP-MS zircon U–Pb ages for sandstone samples of the Yingzuilazi Formation from (A) Yalu River Basin and (B) Liuhe Basin. Data are compiled from Lan (2019) and Pang et al. (2018).

2005 and unpublished data of YQW). The age of the Sainshand suite was suggested to be Aptian to Cenomanian (Khand et al., 2000). *Alicenula*? *dadianziensis* also occurs in the upper part of the Dabeigou Formation (= Dadianzi Formation) (Pang et al., 1984). *Alicenula*? *leguminella* has a long stratigraphic range (Late Jurassic to Albian) and a world-wide distribution (e.g. Wang et al., 2017). A scheme of ostracods stratigraphic ranges from the Yingzuilazi Formation is summarized in Table 3. Consequently, based on the available information above, the age of the Yinzuilaizi Formation is Hauterivian to Barremian, which can be correlated with the Yixian Formation of western Liaoning, the upper part of the Dabeigou Formation (= Dadianzi Formation) in Luanping Basin, the Lower Cretaceous strata from Transbaikalia area of Russia and the Zuunbayan Formation of eastern Mongolia.

5.3. The biota from the Yingzuilazi Formation, and its relationship with Jehol Biota

In addition to a diverse non-marine ostracod fauna, the biota from the Yingzuilazi Formation contains several other animal and plant fossil groups, including conchostracans (clam shrimp), bivalves, gastropods, insects, fishes, amphibians as well as plants like Sphenopsida, Ginkgopsida and Czekanowskiales (see Li et al., 2018, pl. 1; Guo et al., 2018, fig. 3 and references therein). Because of the occurrences of the conchostracan *Eosetheria*, the insect *Ephemeropsis* and the fish *Lycoptera* (EEL assemblage) in the Yingzuilazi Formation as well as sharing several same fossil plant species with the Yixian Formation, the biota from the Yingzuilazi Formation was assigned to the well-known terrestrial Lagersätten Jehol Biota (e.g. Huang, 2016; Li et al., 2018; Guo et al., 2018). However, the definition and distribution pattern of Jehol Biota have been widely discussed since Pan et al. (2013) proposed a new paleoecological definition for this biota integrating the ecological and taphonomic aspects (e.g. Xu et al., 2020; Zhou et al., 2021; Yu et al., 2022b). More recently, Zhou et al. (2021) clearly stated that the poorly defined traditional Jehol Biota is equivalent to the Jehol Biota *sensu lato* as well as the newly defined Jehol Biota by Pan et al. (2013) is named as the Jehol Biota *sensu stricto*. According to Pan et al. (2013), the Jehol Biota *sensu stricto* has a limited paleogeographic distribution in northeast China, occurring in the Huajiying, Yixian and Jiufotang formations in northern Hebei, western Liaoning, and southeast Inner Mongolia (Pan et al., 2013). Whereas, the Jehol Biota *sensu lato* is distributed across the whole of northern China and neighboring regions in eastern and central Asia, which is charactered by occurrences of conchostracan *Eosetheria*, the insect *Ephemeropsis* and the fish *Lycoptera* (EEL assemblage) (e.g. Chen, 1988; Xu et al., 2020;

Table 3
Stratigraphical ranges of the ostracod species present in our samples from the Yingzuilazi Formation of the Baishan Basin. Late Jur. = Late Jurassic, Ber. = Berriasian, Val. = Valanginian, Hau. = Hauterivian, Bar. = Barremian, Apt. = Aptian, Alb. = Albian, Late Cre. = Late Cretaceous.

Species name	Late Jur.	Ber.	Val.	Hau.	Bar.	Apt.	Alb.	Late Cre.
Cypridea tubercularis (Pang in Pang et al., 1984)				—	—			
Cypridea bulumensis Sinitsa, 1992	—	—	—	—	—	—	—	
Cypridea beipiaoensis (Cao, 1999)				—	—			
Lycopterocypris infantilis Lübimova, 1956				—	—	—	—	
Rhinocypris jurassica (Martin, 1940)	—	—	—	—	—			
Ziziphocypris linchengensis Su and Li, 1981				—	—			
Timiriasevia principalis Lübimova, 1956		- - ? - -	—	—	—	—	—	- - - - ? - - - -
Alicenula? *leguinella* (Forbes, 1855)	—	—	—	—	—	—	—	
Alicenula? *dadianziensis* (Pang in Pang et al., 1984)				—	—			

Zhou et al., 2021, fig. 1 and references therein). However, the distribution patter of the Jehol Biota *sensu lato* is questionable and challenged by some recent studies (e.g. Pan et al., 2013; Hethke et al., 2018; Yu et al., 2022b). As Pan et al. (2013) argued, fish *Lycoptera* which is one of the main elements from Jehol Biota *sensu lato* is restricted in the Yixian Formation, the fishes from the Jiufotang Formation should be assigned to genus *Jinanichthy* but not *Lycoptera*. Moreover, the species diversity of Spinicaudata (conchostracan) in the Jehol Biota *sensu lato* has been overestimated and a thorough taxonomic revision of Jehol Biota "*Eosetheria*" fauna is requested (Hethke et al., 2018). Because of lacking detailed taxonomy study on fossil fish and Spinicaudata (conchostracan) of the Yingzuilazi Formation, therefore, the biota from the Yingzuilazi Formation of the Baishan Basin is now better treated as a separate biota from the Jehol Biota *sensu stricto* as well as the Jehol Biota *sensu lato*.

In addition, the newly obtained isotopic ages of the Jehol fossil-bearing stratigraphic units have significantly refined our understanding of the temporal distribution of the Jehol Biota *sensu stricto* (Yang et al., 2020; Zhong et al., 2021; Zhou et al., 2021). This biota has been placed between ~135 Ma and ~120 Ma, that is, during Late Valanginian to Early Aptian (Yang et al., 2020; Zhou et al., 2021). According to Zhou et al. (2021), the Jehol Biota *sensu stricto* is generally divided into three evolving stages, i.e., Jehol Biota stages I (JBS I; ~135 Ma to 127 Ma), JBS II (~126 Ma to ~124 Ma), and JBS III (124 Ma to 120 Ma). Similar to Jehol Biota *sensu stricto*, the biota from the Yingzuilazi Formation was also recovered from the volcaniclastic lacustrine deposits in the NCC. And our new radiometric age suggests that the biota from the Yingzuilazi Formation is probably time consistent with the JBS I defined by Zhou et al. (2021). However, the comprehensive biostratigraphy data and fossil compositions implicate that the biota from the Yingzuilazi Formation can be relative with the JBS II. Therefore, the study of biota from the Yingzuilazi Formation will not only help reveal the spatiotemporal distribution, diversity, and pattern of radiation of the Early Cretaceous terrestrial biome in northeastern China, but also help better understand the linkage of terrestrial life evolution and the deep dynamic processes in the NCC even in East Asia.

6. Conclusions

The Yingzuilazi Formation in the Baishan Basin holds an ostracod fauna consisting of fifteen species belonging to seven genera, *Cypridea tubercularis*, *Cypridea horni* sp. nov., *C. bulumensis*, *C.* aff. *multispinosa*, *C.* cf. *unicostata*, *C. beipiaoensis*, *Rhinocypris jurassica*, *Rhinocypris* sp., *Djungarica* sp., *Ziziphocypris linchengensis*, *Lycopterocypris infantilis*, *L. debilis*, *Timiriasevia principalis*, *Alicenula*? *dadianziensis*, and *Alicenula*? *leguminella*, which were taxonomically studied in detail. This recovered ostracod fauna is relatively unique and diverse, with one new species having been described. Based on the ostracod biostratigraphic correlations, the age of the Yingzuilazi Formation is Hauterivian to Barremian. This age, combined with our new SIMS zircon U–Pb age of 128.5 ± 1.0 Ma for the upper part of the Yingzuilazi Formation, indicates that the age of biota from the Yingzuilazi Formation is mainly Barremian (~129 Ma to ~127 Ma). Considering the chronology and paleontology compositions of the biota from the Yingzuilazi Formation, this biota is treated as a separate biota from the Jehol Biota *sensu lato* as well as the Jehol Biota *sensu stricto*. Although this biota is time consistent with Jehol Biota *sensu stricto* stage I, however, the comprehensive biostratigraphy data and paleontology compositions of this biota implicate that this biota has a close relationship with the Jehol Biota *sensu stricto* stage II. Therefore, this biota will eventually help to not only elucidate the spatiotemporal evolution of the Early Cretaceous terrestrial biotas in East Asia, but also explore the possible relationship between the terrestrial life evolution and the destruction processes of the North China Craton.

Acknowledgments

We would like to thank PhD students Siyuan Ma and Jiajun Mo (GIGCAS) for their assistance in the field, Baoyan Jia (NIGPAS) and Zichen Ge (CDUT) for their technical assistance. Many thanks go to Dr. Yunfeng Li (Jilin University) who provides the measured section data. We also acknowledge the chief editor Dr. Eduardo Koutsoukos and two anonymous reviewers for their constructive comments. Financial support for this study as received from the National Natural Science Foundation of China (Grant No. 42288201, 41688103, 41873018), the Strategic Priority Research Program of the Chinese Academy of Sciences (XDB26000000), and Youth Innovation Promotion Association, CAS (2019309) (YQW).

References

Anderson, F.W., 1941. Ostracoda from the Portland and Purbeck beds at Swindon. Proceedings of Geologists' Association 51, 373–384.

Anderson, F.W., 1985. Ostracod faunas in the Purbeck and Wealden of England. Journal of Micropalaeontology 4 (2), 1–68.

Antonietto, L.S., Park Boush, L.E., Suarez, C.A., Milner, A.R.C., Kirkland, J.I., 2018. The 'Last Hurrah of the Reigning Darwinulocopines'? Ostracoda (Arthropoda, Crustacea) from the Lower Jurassic Moenave Formation, Arizona and Utah, USA. Journal of Paleontology 92, 648–660.

Ayress, M.A., Whatley, R.C., 2014. Early Cretaceous non-marine Ostracoda from the north Falkland Basin, South Atlantic. Palaeontology 57, 1143–1175.

Baird, W., 1845. Arrangement of the British Entomostraca, with a list of species, particularly noticing those which have as yet been discovered within the bounds of the club. Transactions of the Berwickshire Naturalist's Club 2 (13), 145–158.

Bosquet, J., 1852. Description des Entomostracés Fossiles des Terrains Tertiaires de la France et de la Belgique. Mémoires Couronnés et Mémoires des Savants Étrangers 24, 1–142.

Brady, G.S., Norman, A.M., 1889. A monograph of the marine and freshwater Ostracoda of the North Atlantic and of North Western Europe. I. Podocopa. The Scientific Transactions of the Royal Dublin Society, Series 2 (4), 63–270.

Bureau of Geology and Mineral Resources of Jilin Province, 1988. Regional geology of Jilin Province. Geological Publishing House, Beijing, pp. 1–698 (in Chinese).

Bureau of Geology and Mineral Resources of Jilin Province, 1997. Stratigraphy (Lithostatic) of Jilin Province. China University of Geosciences Press, Wuhan, pp. 1–324 (in Chinese).

Cao, M.Z., 1999. Nonmarine ostracods of the lower part of the Yixian Formation in Sihetun area, western Liaoning, China. Palaeoworld 11, 131–144 (in Chinese, with English abstract).

Chen, D.Q., 1965. The ostracode genus *Metacypris* and its allies. Acta Palaeontologica Sinica 13, 1–28 (in Chinese, with English abstract).

Chen, P.J., 1988. Distribution and migration of Jehol fauna with reference to non-marine Jurassic/Cretaceous boundary in China. Acta Palaeontologica Sinica 27, 659–683 (in Chinese, with English abstract).

Chen, J.S., Li, B., Yao, Y.L., Liu, M., Yang, F., Xing, D.H., Li, W., Wang, Y., 2016. Comparison between Mesozoic volcanic rock strata in Northeast of Liaoning, South of Jilin and Yixian Formation in West of Liaoning. Acta Geologica Sinica 90, 2733–2746 (in Chinese, with English abstract).

Choi, B.D., Wang, Y.Q., Hu, L., Huh, M., 2020. Ostracod faunas from the Dalazi and Tongfosi formations (Yanji Basin, northeast China): Biostratigraphic, palaeogeographic and palaeoecological implications. Cretaceous Research 105, 104018.

Corfu, F., Hanchar, J.M., Hoskin, P.W., Kinny, P., 2003. Atlas of zircon textures. Reviews in Mineralogy and Geochemistry 53, 469–500.

Danielopol, D.L., Cabral, M.C., Lord, A., Carbonel, P., Gross, M., Stoica, M., Humphreys, W.F., Namiotko, T., Tóth, E., Külköylüoğlu, O., Piller, W.E., Nunes, T., 2018. Sieve-type pore canals in the Timiriaseviinae – a contribution to the comparative morphology and the systematics of the Limnocytheridae (Ostracoda, Crustacea). Zootaxa 4495 (1), 1–64.

Egger, J.R., 1910. Ostracoden und Foraminiferen des Eybrunner Kreidemergels in der Umgebung von Regensburg. Berichte des Naturwissenschaftlichen Verein Regensburg 12, 86–126.

Feng, Y.Z., Yang, J.H., Sun, J.F., Zhang, J.H., 2020. Material records for Mesozoic destruction of the North China Craton by subduction of the Paleo-Pacific slab. Science China Earth Sciences 63, 690–700 (in Chinese, with English abstract).

Forbes, E., 1855. Middle Purbeck, Lower Purbeck. In: Lyell, C. (Ed.), Manual of Elementary Geology, fifth ed. John Murray, London, pp. 94–297.

Galeeva, L.I., 1955. Ostracody Melovykh Otlozheniy Mongolskoy Narodnoy Respubliki (Ostracoda from Cretaceous Deposits of the People's Republic of Mongolia). Gostoptekhizdat, Moskva, p. 97 (in Russian).
Gou, Y.X., Wang, Z.Z., Yang, J.D., Wang, W.S., 1986. Cretaceous ostracods from Eren Basin of Nei Mongol along with sedimentary environments. In: Nanjing Institute of Geology and Palaeontology, Chinese Academy of Sciences, North China Petroleum Administration Bureau. Cretaceous Ostracod and Sporo-Pollen Fossils of Eren Basin, Nei Mongol. Anhui Science and Technology Publishing House, Hefei, pp. 1–93 (in Chinese).
Guo, L.N., Liu, W.Z., Su, B., Li, T., Li, Y.F., 2018. Determination of Lower Cretaceous Yingzuilazi Formation in Baishan Basin in southeastern Jilin, China and its geological significance. Global Geology 37, 665–674 (in Chinese, with English abstract).
Hethke, M., Fürsich, F.T., Morton, J., Jiang, B.Y., 2018. Analysis of morphological variability in the clam shrimp *Eosestheris middendorfii* (Crustacea, Spinicaudata) from the Lower Cretaceous of China, and its implications for spinicaudatan taxonomy. Paper in Palaeontology 4, 21–53.
Horne, D.J., 2005. Ostracoda. In: Selley, R.C., Cocks, R.M., Plimer, I.R. (Eds.), Encyclopedia of Geology. Elsevie, Oxford, pp. 453–463.
Hou, Y.T., 1958. Jurassic and Cretaceous non-marine ostracods of the subfamily Cyprideinae from north-western and north-eastern regions of China. Memoirs of Nanjing Institute of Geology and Palaeontology. Academia Sinica 1, 32–103.
Hou, Y.T., Gou, Y.X., Chen, D.Q., 2002. Fossil Ostracoda of China, Vol. 1e Superfamilies Cypridacea and Darwinulidacea. Science Press, Beijing, p. 1090 (in Chinese).
Huang, Y.Q., 1985. Mesozoic-Cenozoic ostracodes from the Hetao Area in Inner Mongolia. In: Selected Paper on Micropalaeontology of China. Science Press, Beijing, pp. 119–130 (in Chinese).
Huang, W., 2016. The discovery of Jehol Biota and fossil plants from southeastern Jilin, China (PhD thesis). Jilin University, p. 203 (in Chinese).
Huang, C., Wang, H., Yang, J.H., Ramezani, J., Yang, C., Zhang, S.B., Yang, Y.H., Xia, X.P., Feng, L.J., Lin, J., Wang, T.T., Ma, Q., He, H.Y., Xie, L.W., Wu, S.T., 2020. SA01 – a proposed zircon reference material for microbeam U-Pb age and Hf-O isotopic determination. Geostandards and Geoanalytical Research 44 (1), 103–123.
Kaufmann, A., 1900. Cypriden und Darwinuliden der Schweig. Revue Suissede Zoologie. Annales de la Société Zoologique de Suisse 8, 209–423 (in German).
Khand, Y., Badamgarav, D., Ariunchimeg, Y., Barsbold, R., 2000. Cretaceous system in Mongolia and its depositional environments. In: Okada, H., Mateer, N.J. (Eds.), Cretaceous Environments of Asia, Developments in Palaeontology and Stratigrahpy, vol. 17, pp. 49–79.
Klie, W., 1935. Ostracoda aus dem tropischen Westafrica. Archiv für Hydrobiologie 28, 35–68.
Lan, Y.Z., 2019. Research on sedimentary and reservior developmental characteristics of Early Cretaceous Yingzuilazi Formation in Liuhe Basin (Master thesis). Jilin University, p. 90 (in Chinese).
Latreille, P.A., 1802. Cenera Crustaceorum et Insectorum. Tomus Primus. A. Koenig, Paris, p. 302.
Li, H.R. (Ed.), 1989. Mesozoic Ostracoda Fauna from Eren Basin, Inner Mongolia. Petroleum Industry Press, Beijing, p. 97 (in Chinese).
Li, C.W., 2006. Petrogenesis and geological implications of the late Mesozoic volcanic rocks in southeastern Jilin province, northeastern China (PhD thesis). Graduate School of The Chinese Academy of Sciences, p. 134 (in Chinese).
Li, X.H., Liu, Y., Li, Q.L., Guo, C.H., Chamberlain, K.R., 2009. Precise determination of Phanerozoic zircon Pb/Pb age by multicollector SIMS without external standardization. Geochemistry, Geophysics, Geosystems 10, 1–21.
Li, C.W., Guo, F., Fan, W.M., 2011. Lower crustal melting via magma underplating: Elemental and Sr–Nd–Pb isotopic constraints from late Mesozoic intermediate–felsic volcanic rocks in the northeastern North China Block. Island Arc 20 (4), 477–499.
Li, Y.F., Sun, C.L., Li, T., Na, Y.L., Chen, Y.J., Xing, D.D., 2015. *Solenites* (Czekanowskiales) from the Late Mesozoic Jehol Biota of Southeastern Jilin, China and its paleoclimatic implications. Acta Geologica Sinica 89, 1088–1102.
Li, Y.F., Huang, W., Wang, H.S., Dilcher, D.L., Tan, X., Li, T., Na, Y.L., Sun, C.L., 2018. The first discovery of the easternmost Jehol Biota from southeastern Jilin, China. Acta Geologica Sinica 92, 1649–1650.
Liu, X.S., Li, W., Zhang, M.S., Zhao, H.M., 2018. Geochronology and geological significance of Early Cretaceous volcanic rocks from Guosong Formation in Guosong Basin, Jilin. Global Geology 37 (1), 37–45 (in Chinese, with English abstract).
Lübimova, P.S., 1956. Ostracody Melovykh Otlozheniy Vostochnoy Chasti-Mongolskoy 878 Narodnoy Respubliki i ikh Znachenie dlya Stratigrafii [Ostracoda from Cretaceous deposits of 879 the eastern part of the People's Republicof Mongolia and their significance for stratigraphy]. 880 Trudy Vsesoyuzno-goNeftyanogo Nauchno–Issledovatelskogo Geologo – Razvedochnogo 881 Insti-tuta (VNIGRI), Novaya Seriya 93, 1–174 (in Russian).
Ludwig, K.A., 2011. Isoplot/Ex, Version 4.15: a geochronological toolkit for Microsoft Excel, vol. 4. Berkeley Geochronology Center Special Publication.
Mandelstam, M.I., 1947. Ostracoda iz otlozheniy Sredney Yuri Poluostrova Mangyshlaka (Ostracoda from Middle Jurassic deposits of the Mangish-lak peninsula). In: Mikrofauna Neftyanykh Mestorozhdeniy Kavkasa, Emby iSredney Azii. VNIGRI, Moscow/Leningrad, pp. 239–259 (in Russian).
Mandelstam, M.I., 1960. In: Kashevarova, N.P., Mandelstam, M.I. and Schneider, G.F. Ostracoda: Nadsemeystvo Cytheracea. In: Orlov, Y.A (Ed.), Osnovy Paleontologii. Moskva: Gosudarstvennoe Nauchno–Technicheskoe Isdatelstvo Literaturiy po Geologii i Ochrane Nedra 8, 365–411 (in Russian).
Martens, K., Rossetti, G., Horne, D.J., 2003. How ancient are ancient asexuals? Proceedings of the Royal Society B: Biological Sciences 270, 723–729.
Martin, G.P.R., 1940. Ostracoden des norddeutschen Purbeck und Wealden. Senckenbergiana 22, 275–361.
Meisch, C., Smith, R.J., Martens, K., 2019. A subjective global checklist of the extant non-marine Ostracoda (Crustacea). European Journal of Taxonomy 492, 1–135.
Meng, Q.R., Zhou, Z.H., Zhu, R.X., Xu, Y.G., Guo, Z.T., 2021. Cretaceous basin evolution in Northeast Asia: Tectonic responses to the paleo-Pacific plate subduction. National Science Review 9, nwab088.
Nanjing Institute of Geology and Palaeontology, Chinese Academy of Sciences, 1963. Index Fossil Handbook of Northwest China. Science Press, Beijing, p. 163 (in Chinese).
Neustrueva, I.Y., Sinitsa, S.M., Khand, Y., Melnikova, L.M., 2005. Paleontologia Mongolii. Posdnemesosoiskye i Paleogenovye Ostrakody (Paleontology of Mongolia: Late Mesozoic and Paleogene Ostracods). Nauka, Moskva, p. 166 (in Russian).
Pan, Y.H., Sha, J.G., Zhou, Z.H., Fürsich, F.T., 2013. The Jehol Biota: definition and distribution of exceptionally preserved relicts of a continental Early Cretaceous ecosystem. Cretaceous Research 44, 30–38.
Pang, Q.Q., 1978. Late Mesozoic ostracods from the Guyang Group and its implication on biostratigraphy, Central Inner Mongolia. Journal of Hebei GEO University 3, 56–79 (in Chinese).
Pang, Q.Q., 1979. Cretaceous ostracods from the Central Inner Mongolia. Journal of Hebei GEO University 2, 30–54 (in Chinese).
Pang, Q.Q., 1982. Ostracoda. In: Inner Mongolia Bureau of Geology (Ed.), The Mesozoic stratigraphy and paleontology of Guyang coal-bearing Basin Neimenggol Autonomous Region. Geological Publishing House, China. Beijing, pp. 57–84 (in Chinese).
Pang, Q.Q., Zhang, L.X., Wang, Q., 1984. Ostracoda. In: Tianjin Institute of Geology and Mineral Resources (Ed.), Palaeontological Atlas of North China, 3 Micropalaeontological Volume. Geological Publishing House, Beijing, pp. 59–84.
Pang, X.W., Wang, Y.N., Zhang, M.S., Li, X.B., Liu, X.S., Luan, J.P., 2018. Depositional age and provenances of Yingzuilazi Formation and Mantou Formation in Yalu River Basin: evidence from U-Pb ages of detrital zircons. Global Geology 37 (2), 385–398 (in Chinese, with English abstract).
Pei, F.P., 2005. Petrology and Geochemistry of Mesozoic Volcanic Rocks in Southern Jilin Province (Master thesis). Jilin University, p. 88 (in Chinese).
Rossetti, G., Martens, K., 1998. Taxonomic revision of the recent and holocene representatives of the family Darwinulidae (Crustacea, Ostracoda), with a description of three new genera. Bulletin de L'Institut Royal des Sciences Naturelles de Belgique, Biology 68, 55–110.
Sames, B., 2011a. Early Cretaceous *Cypridea* Bosquet 1852 in North America and Europe. In: Sames, B. (Ed.), Taxonomic Studies in Early Cretaceous Nonmarine Ostracoda of North America, Micropaleontology, vol. 57 (4–5), pp. 291–344.
Sames, B., 2011b. Early Cretaceous *Theriosynoecum* Branson 1936 in North America and Europe. In: Sames, B. (Ed.), Taxonomic Studies in Early Cretaceous Nonmarine Ostracoda of North America, Micropaleontology, vol. 57 (4–5), pp. 345–431.
Sames, B., 2011c. Glossary of morphologic terms of late Mesozoic nonmarine Ostracoda, relevant to *Theriosynoecum* Branson 1936 and *Cypridea* Bosquet 1852. In: Sames, B. (Ed.), Taxonomic Studies in Early Cretaceous Nonmarine Ostracoda of North America, Micropaleontology, vol. 57 (4–5), pp. 433–454.
Sames, B., Horne, D.J., 2012. Latest Jurassic to Cretaceous non-marine ostracod biostratigraphy: unde venis, quo vadis? Journal of Stratigraphy 3T6, 267–288.
Sars, G.O., 1866. Oversigt af Norges marine Ostracoder. Forhandliger I Videnskabs-Selskabet I Christiana 1865, Christiania.
Sars, G.O., 1928. Ostracoda. In: Sars, G.O. (Ed.), An account of the Crustacea of Norway with short descriptions and figures of all the species, vols. 6, 9 (15–16). Bergen Museum, Bergen, Annex, Corrections, pp. 241–271.
Schudack, U., Schudack, M., 2012. Non-*Cypridea* Ostracoda from the Lower Cretaceous of the Iberian Chain (Spain). Neues Jahrbuch für Geologie und Paläontologie - Abhandlungen 266 (3), 251–271.
Sha, J.G., 2007. Cretaceous stratigraphy of northeast China: non-marine and marine correlation. Cretaceous Research 28, 146–170.
Sinitsa, S.M., 1973. New Late Mesozoic Ostracoda from Transbaikalia (Novye Pozdnemezozoyskie Ostrakody Zabaykalya). Zapiski Zabaykalskogo Filiala Geograficheskogo Osbshchestva SSSR 14, 103–117 (in Russian).
Sinitsa, S.M., 1992. New Ostracoda from Jurassic and Lower Cretaceous deposits of eastern Transbaikalia (Novye Ostrakody Iz Yurskikh I Nizhnemeloveykh Otlozheniy Vostochnogo Zabaykalya). Paleontologicheskiy Zhurnal 3, 20–33 (in Russian, with English abstract).
Sinitsa, S.M., 1993. Jurassic and Lower Cretaceous of Central Mongolia: ostracoda, stratigraphy and palaeoreconstruction. Trudy. Sovmestnaya Sovetsko-Mongolskaya Paleontologicheskaya Ekspeditsiya 42, 1–236.
Sláma, J., Košler, J., Condon, D.J., et al., 2008. Plešovice zircon—a new natural reference material for U–Pb and Hf isotopic microanalysis. Chemical Geology 249 (1–2), 1–35.
Sowerby, J.D.C., 1836. Descriptive notes respecting the shells figured in plates XI to XXI. In: Fitton, W.H. (Ed.), Observation on some of the strata between the Chalk and the Oxford Oolithe. The Geological Society, London, pp. 344–345.
Su, D.Y., Li, Y.G., 1981. Ostracods from the Lincheng Formation at the eastern foot of Taihang Mountain and their geological age. Bulletin of the Institute of Geology, Chinese Academy of Geological Sciences 3, 120–126 (in Chinese, with English abstract).

Tomé, E.T.R.M., Filho, F.L.M., Neumann, H.M.L.V., 2014. Taxonomic studies of non-marine ostracods in the Lower Cretaceous (Aptian–lower Albian) of post-rift sequence from Jatobá and Araripe basins (Northeast Brazil): Stratigraphic implications. Cretaceous Research 48, 153–176.
Trabelsi, T., Sames, B., Nasri, A., Piovesan, E.K., Elferhi, F., Skanji, A., Houla, Y., Soussi, M., Wagreich, M., 2020. Ostracod as proxies for marginal marine to non-marine intervals in the mid-Cretaceous carbonate platform of the Central Tunisian Atlas (North Africa): Response to major short-term sea-level falls. Cretaceous Research 117, 104581.
Van Itterbeeck, J., Markevich, V.S., Horne, D., 2004. The age of the dinosaur-bearing Cretaceous sediments at Dashuiguo, Inner Mongolia, P.R. China based on charophytes, ostracods and palynomorphs. Cretaceous Research 25, 391–409.
Wang, Y.Q., Sha, J.G., Pan, Y.H., 2013. Revision of *Cypridea* (non-marine Ostracoda) from the Early Cretaceous Yixian Formation of the Beipiao-Yixian Basin in western Liaoning, northeast China. Cretaceous Research 40, 102–109.
Wang, Y.Q., Sha, J.G., Pan, Y.H., Zhang, X.L., 2015. Early Cretaceous nonmarine ostracod biostratigraphy of western Liaoning area NE China. Micropaleontology 61, 135–145.
Wang, Y.Q., Sha, J.G., Pan, Y.H., Zuo, Q.M., 2016. The Early Cretaceous non-*Cypridea* Ostracoda from Yixian and Jiufotang formations of western Liaoning (China). Palaeoworld 25, 406–424.
Wang, Y.Q., Yang, W.G., Pan, Y.H., Liao, H.Y., 2017. Species of the genus *Cypridea* Bosquet, 1852 (Ostracoda) from the Lower Cretaceous Yixian and Jiufotang formations of western Liaoning, China. Palaeoworld 26, 339–351.
Whitehouse, M.J., Claesson, S., Sunde, T., Vestin, J., 1997. Ion microprobe U-Pb zircon geochronology and correlation of Archaean gneisses from the Lewisian Complex of Gruinard Bay, northwestern Scotland. Geochimica et Cosmochimica Acta 61, 4429–4438.
Xi, D.P., Wan, X.Q., Li, G.B., Li, G., 2019. Cretaceous integrative stratigraphy and timescale of China. Science China Earth Sciences 62, 256–268.
Xin, H.T., Niu, S.W., Wang, H.C., Yuan, G.B., 2000. New progress in the study of the Lower Cretaceous of the Guyang area, Inner Mongolia. Regional Geology of China 19, 361–366 (in Chinese, with English abstract).
Xu, X., Zhou, Z.H., Wang, Y., Wang, M., 2020. Study on the Jehol Biota: Recent advances and future prospects. Science China Earth Sciences 63, 757–773.
Yang, S.H., He, H.Y., Jin, F., Zhang, F.C., Wu, Y.B., Yu, Z.Q., Li, Q.L., Wang, M., O'Connor, J.K., Deng, C.L., Zhu, R.X., Zhou, Z.H., 2020. The appearance and duration of the Jehol Biota: Constraint from SIMS U-Pb zircon dating for the Huajiying Formation in northern China. Proceedings of the National Academy of Sciences of the United States of America 117, 14299–14305.
Ye, C.H., Gou, Y.X., Hou, Y.T., Cao, M.Z., 1977. Mesozoic–Cenozoic ostracode fauna from Yunnan. In: Nanjing Institute of Geology and Palaeontology, Chinese Academy of Science (Ed.), Divisions and Correlations of the Mesozoic Volcano-Sedimentary Formations in Zhejiang and Anhui Provinces, vol. 2. Science Press, Beijing, pp. 153–330 (in Chinese).
Yu, Z.Q., Dong, L.P., Huyskens, M.H., Yin, Q.Z., Wang, Y., Deng, C.L., He, H.Y., 2022b. The exceptionally preserved Early Cretaceous "Moqi Fauna" from eastern Inner Mongolia, China, and its age relationship with the Jehol Biota. Palaeogeography, Palaeoclimatology, Palaeoecology 589, 110824.
Yu, Z.Q., Qin, Z.H., Xi, D.P., Deng, C.L., He, H.Y., Zhou, Z.H., 2022a. New geochronology of the Lower Cretaceous in the Luanping Basin, northern Hebei: age constraints on the development of early Jehol Biota. Palaeogeography, Palaeoclimatology, Palaeoecology 568, 110768.
Zhang, L.J., 1985a. Ostracods. In: Zhang, L.J., Wu, R.P., Wu, H.Z. (Eds.), Mesozoic Stratigraphy and Palaeontology of Western Liaoning. Geological Publishing House, Beijing, pp. 1–120 (in Chinese).
Zhang, L.J., 1985b. The freshwater ostracodes from the Lower Cretaceous Jiufotang and Shahai formations in the Western Liaoning. In: Selected Paper on Micropalaeontology of China. Science Press, Beijing, pp. 137–149 (in Chinese).
Zhao, L., 2015. Study on the geochronology of Mesozoic volcanic rocks in Huanren, Liaoning and Tonghua, Jilin (Master thesis). Jilin University, p. 82 (in Chinese).
Zhao, M., Sun, C.L., Dilcher, D.L., Na, Y.L., Xing, D.H., 2016. A new species of *Baiera* from the Early Cretaceous Jehol Biota of southeastern Jilin, China. Palaeoworld 25, 251–262.
Zhong, Y.T., Huyskens, M.H., Yin, Q.Z., Wang, Y.Q., Ma, Q., Xu, Y.G., 2021. High-Precision Geochronological Constraints on the Duration of 'Dinosaurs Pompeii' and the Yixian Formation. National Science Review, 0, nwab063.
Zhou, H., 2021. Petrogenesis of Early Cretaceous volcanic rocks of the southern Jilin Province and Liaodong Peninsula: Constraints from elemental and Sr-Nd-Pb isotope geochemistry (PhD thesis). Jilin University, p. 172 (in Chinese).
Zhou, Z.H., Wang, Y., 2017. Vertebrate assemblages of the Jurassic Yanliao Biota and the Early Cretaceous Jehol Biota: Comparisons and implications. Palaeoworld 26, 241–252.
Zhou, Z.H., Meng, Q.R., Zhu, R.X., Wang, M., 2021. Spatiotemporal evolution of the Jehol Biota: Responses to the North China craton destruction in the Early Cretaceous. Proceedings of the National Academy of Sciences of the United States of America 118, e2107859118.
Zhu, R.X., Xu, Y.G., Zhu, G., Zhang, H.F., Xia, Q.K., Zheng, T.Y., 2012a. Destruction of the North China Craton. Science China Earth Sciences 55, 1565–1587.
Zhu, R.X., Yang, J.H., Wu, F.Y., 2012b. Timing of destruction of the North China Craton. Lithos 149, 51–60.
Zhu, R.X., Zhou, Z.H., Meng, Q.R., 2020. Destruction of the North China Craton and its influence on surface geology and terrestrial biotas. Chinese Science Bulletin 65, 2954–2965 (in Chinese, with English abstract).

Appendix A. Supplementary data

Supplementary data to this article can be found online at https://doi.org/10.1016/j.cretres.2022.105275.